VERIFICATION OF RESPONSE SPECTRAL SHAPES AND ANCHOR POINTS FOR DIFFERENT SITE CATEGORIES IN BUILDING DESIGN CODES

by

Walt Silva

Pacific Engineering and Analysis
El Cerrito, California

and

Gabriel Toro

Risk Engineering
Boulder, Colorado

Data Utilization Report CSMIP/00-06 (OSMS 00-08)

California Strong Motion Instrumentation Program

March 2000

CALIFORNIA DEPARTMENT OF CONSERVATION
DIVISION OF MINES AND GEOLOGY
OFFICE OF STRONG MOTION STUDIES

THE RESOURCES AGENCY
MARY NICHOLS
SECRETARY FOR RESOURCES

STATE OF CALIFORNIA
GRAY DAVIS
GOVERNOR

DEPARTMENT OF CONSERVATION
DARRYL YOUNG
DIRECTOR

DIVISION OF MINES AND GEOLOGY
JAMES F. DAVIS
STATE GEOLOGIST

DISCLAIMER

The content of this report was developed under Contract No. 1093-552 from the Strong Motion Instrumentation Program in the Division of Mines and Geology of the California Department of Conservation. This report has not been edited to the standards of a formal publication. Any opinions, findings, conclusions or recommendations contained in this report are those of the authors, and should not be interpreted as representing the official policies, either expressed or implied, of the State of California.

VERIFICATION OF RESPONSE SPECTRAL SHAPES AND ANCHOR POINTS FOR DIFFERENT SITE CATEGORIES IN BUILDING DESIGN CODES

by

Walt Silva

Pacific Engineering and Analysis
El Cerrito, California

and

Gabriel Toro

Risk Engineering
Boulder, Colorado

Data Utilization Report CSMIP/00-06 (OSMS 00-08)

California Strong Motion Instrumentation Program

March 2000

This study was conducted at the Pacific Engineering and Analysis in El Cerrito, California from June 1994 to June 1996 and was supported by the Department of Conservation under Contract No. 1093-552.

California Department of Conservation
Division of Mines and Geology
Office of Strong Motion Studies
801 K Street, MS 13-35
Sacramento, California 95814-3531

PREFACE

The California Strong Motion Instrumentation Program (CSMIP) in the Division of Mines and Geology of the California Department of Conservation promotes and facilitates the improvement of seismic codes through the Data Interpretation Project. The objective of the this project is to increase the understanding of earthquake strong ground shaking and its effects on structures through interpretation and analysis studies of CSMIP and other applicable strong motion data. The ultimate goal is to accelerate the process by which lessons learned from earthquake data are incorporated into seismic code provisions and seismic design practices.

The specific objectives of the CSMIP Data Interpretation Project are to:

1. Understand the spatial variation and magnitude dependence of earthquake strong ground motion.

2. Understand the effects of earthquake motions on the response of geologic formations, buildings and lifeline structures.

3. Expedite the incorporation of knowledge of earthquake shaking into revision of seismic codes and practices.

4. Increase awareness within the seismological and earthquake engineering community about the effective usage of strong motion data.

5. Improve instrumentation methods and data processing techniques to maximize the usefulness of SMIP data. Develop data representations to increase the usefulness and the applicability to design engineers.

This report is part of CSMIP data utilization reports designed to transfer recent research findings on strong-motion data to practicing seismic design professionals and earth scientists. CSMIP extends its appreciation to the members of the Strong Motion Instrumentation Advisory Committee and its subcommittees for their recommendations regarding the Data Interpretation Research Project.

Anthony F. Shakal
CSMIP Program Manager

Moh J. Huang
CSMIP Data Interpretation
Project Manager

ABSTRACT

The dramatic increase in strong ground motion recordings over the last several years has provided both the impetus and opportunity to empirically examine the seismic design criteria in both the UBC 94 and NEHRP 94 code provisions. In this project both spectral design shapes and the usefulness of two spectral anchors are investigated using a comprehensive strong motion database and updated empirical attenuation relations. For the shapes, comparisons with statistical shapes with mean magnitudes in the range of 6.6 to 6.9 to design shapes suggest that both the UBC 94 and NEHRP 94 design spectra provide enveloping criteria (except for site D at short periods) including cases for sites within 10 km of the fault rupture surface. For the NEHRP 94 design spectra, comparison of the F_a and F_v factors to those implied by a recently developed empirical attenuation relation suggest that the NEHRP 94 F_a factors may reflect too little nonlinearity while the F_v factors may show too much nonlinearity. Comparisons of the code shapes to the results from probabilistic seismic hazard analyses indicate that the fixed UBC 94 shape has a moderate tendency to under-predict amplitudes for $T \geq 1$ sec in places like San Francisco where large ($M > 7$) earthquakes dominate the hazard at these periods. The more flexible NEHRP 94 shape avoids this problem, but requires the appropriate specification of two anchoring points.

APPLICATION TO CODES AND PRACTICES

Recent revisions to the National Earthquake Hazard Reduction Program (NEHRP 94) site amplification factors for base shear coefficients has resulted in a revised set of site categories and a set of both short and intermediate-to-long period site factors. The new site factors accommodate nonlinear site effects through a dependency on soft rock effective accelerations. Unlike the UBC 94 site factors, these revised factors were largely based on model calculations as insufficient strong motion data were available at the higher ground motion levels. Recent substantial increases in the number of data, particularly at high levels of motion, has presented the opportunity to empirically assess the revised spectral design shapes as well as the use of the two anchor points to set the design levels. The results suggest that both the UBC 94 and NEHRP 94 design spectra provide enveloping criteria (except for site category D at short periods) including cases for close-in sites ($\leq$ 10 km) for earthquakes in the magnitude range of 6.6 to 6.9. Direct evaluation of the short and intermediate-to-long period amplification factors indicate that the degree of nonlinearity captured in the factors may not reflect that of the empirical data base.

Comparisons of code design spectra to results from probabilistic seismic hazard analyses indicate that the UBC 94 shape underpredicts intermediate-to-long period motions ($T \geq 1$ sec) in areas such as San Francisco where large magnitude ($M > 7$) earthquakes dominate the hazard. The revised shapes (NEHRP 94), using two anchor points, provide a better representation of the shaking hazard than does a single anchor point but only if both anchoring values are appropriately specified.

ACKNOWLEDGMENTS

This investigation was funded by the Strong Motion Instrumentation Program, California Division of Mines and Geology. The authors are grateful for this support and wish to thank all members of the SMIP project committee for their very useful comments during the project. We also thank the reviewers for their constructive reviews which greatly improved the report as well as Dr. Moh Hwang for his patience and guidance. A special thanks to Dr. Mark Petersen, also of CDMG, for providing information on the seismic-source characterization for Los Angeles.

TABLE OF CONTENTS

INTRODUCTION

Local geologic conditions have long been recognized to have a large effect upon strong ground motions. Del Barrio, in the 1855 Proceedings of the University of Chile states[1] "...a movement... must be modified while passing through media of different constitutions. Therefore, the earthquake effects will arrive to the surface with higher or lesser violence according to the state of aggregation of the terrain which conducted the movement. This seems to be, in fact, what we have observed in the Colchagua Province (of Chile) as well as in many other cases". The stable variations in spectral content for different site conditions give rise to site dependent ground motion characteristics which result from vertical variations in soil properties (Mohraz, 1976; Seed et al., 1976). These effects have been incorporated into building codes in the United States (UBC; NEHRP, 1991) as well as elsewhere (IAEE, 1992) as site category dependent response spectral shapes. The UBC 94 site categories (Table 1) and shape coefficients were developed primarily during the ATC-3 effort in the early to mid 1970's and reflect the state of knowledge at that time. Site categories S_1 to S_3 were developed by Seed et al. (1976) and category S_4 was added subsequent to the 1985 Mexico City earthquake to accommodate deep soft (clay) profiles. The site coefficients corresponding to the S_1 to S_4 site categories affect only the intermediate-to-long period portion of the spectrum (range of approximately constant response spectral velocity) as insufficient data were available to resolve stable features of short period site dependent response. It is important to point out that site dependent spectral shapes reflected in the code provision not only represent ground response spectra, but also accommodate judgmental factors for structural engineering considerations, such

[1]Translated from the old Spanish by Professor Ricardo Dobry.

as a factor of 1.25 along with a $T^{2/3}$ fall-off at long periods. Both the 1997 UBC and 1997 NEHRP have adopted a T^{-1} shape for lateral force provisions. In addition, the 1997 UBC has also adopted the NEHRP site coefficients.

Subsequent to the 1989 Loma Prieta earthquake and the accompanying dramatic increase of data on site effects, the need was recognized for an update of the code-provision site factors. This effort was undertaken by a number of practitioners and culminated in a consensus (1992 NCEER/SEAOC/BSSC/Workshop) set of revised site categories (A to F, Table 1) and a set of both short period (F_a) and intermediate-to-long period (F_v) site factors applied to the soft rock (Category B) shape. The new site factors accommodate nonlinear site effects through a dependency on soft rock acceleration and velocity based effective accelerations (A_a and A_V, Table 2).

The revised site categories are more quantative, being based on the average shear-wave velocity over the top 100 ft of material below the surface. The number of categories have been increased as well from 4 to 5, with the very hard rock category (A in Table 1) added to specifically address rock site conditions more typical of the central and eastern United States.

Because the UBC 94 spectra were developed in the early to mid 1970's and the NEHRP 94 recommended revisions are based primarily on site response analyses and limited empirical analyses for rock peak accelerations less than about 0.10 to 0.15g (Seed and Dickenson, 1993; Borcherdt, 1994) the increase in strong motion data over the last several years provides an important empirical check on these design requirements. The purpose of this project is to

provide an empirical check on the 1994 UBC and 1994 NEHRP code provisions design response spectral shapes using currently available large magnitude ($M \geq 6.3$) strong motion recordings binned into appropriate site categories. The second part of this report uses probabilistic seismic hazard analysis (PSHA) calculations for selected California cities, calculates uniform-hazard spectra for 90% non-exceedence probability in 50 years, and compares these spectra to the code provisions. The purposes of these calculations and comparisons are as follows: (1) investigate the benefits of using two spectral anchor points (short and intermediate-period), (2) investigate the effect of increased uncertainty in long-period attenuation equations on spectral shapes (and whether this might require code shapes that decay slower than T^{-1}), (3) determine the magnitudes-distance combinations that dominate seismic hazard for 90% non-exceedence probability in 50 years (thus guiding the selection of magnitudes and distances to use in constructing the statistical shapes), and (4) provide a check on the absolute levels (or anchor points) used in the UBC 94 and NEHRP 94 code provisions.

Table 1
PROFILE TYPES

UBC 94

Soil Profile Type	Description	Soil Factors	
		S'	S'
S_1	A soil profile with either: (1) rock of any characteristic, either shale-like or crystalline in nature, that has a shear wave velocity greater than 2,500 feet per second or (2) stiff soil conditions where the soil depth is less than 200 feet and the soil types overlying the rock are stable deposits of sands, gravels, or stiff clays.	1.00	1.00
S_2	A soil profile with deep cohesionless or stiff clay conditions where the soil depth exceeds 200 feet and the soil types overlying rock are stable deposits of sands, gravels, or stiff clays.	1.20	1.40
S_3	A soil profile containing 20 to 40 feet in thickness of soft- to medium-stiff clays with or without intervening layers of cohesionless soils.	1.50	2.05
S_4	A soil profile characterized by a shear wave velocity of less than 500 feet per second containing more than 40 feet of soft clays or silts.	2.00	**

NEHRP 94 Provisions

A	Hard rock with measured shear wave velocity, $\overline{V_S}$ > 5,000 *ft*/sec
B	Rock with 2,500 *ft*/sec < $\overline{V_S}$ ≤ 5,000 *ft*/sec
C	Very dense soil and soft rock with 1,200 *ft*/sec < $\overline{V_S}$ < 2,500 *ft*/sec
D	Stiff soil with 600 *ft*/sec ≤ $\overline{V_S}$ ≤ 1,200 *ft*/sec
E	A soil profile with $\overline{V_S}$ < 600 *ft*/sec or any profile with more than 10 ft of soft clay
F	Soil requiring site-specific evaluations

Assumed UBC 94 and NEHRP 94 Profile Relationships

UBC Profile	NEHRP Profile
S_1	B and C
S_2	C and D
S_3	E

**Dynamic analyses for buildings on S_4 soils require site specific investigations

Table 2
F_a AND F_v VALUES

Soil Profile Type	F_a For Shaking Intensity Levels				
	$A_a \leq 0.1$	$A_a = 0.2$	$A_a = 0.3$	$A_a = 0.4$	$A_a \geq 0.50^a$
A	0.8	0.8	0.8	0.8	0.8
B	1.0	1.0	1.0	1.0	1.0
C	1.2	1.2	1.1	1.0	1.0
D	1.6	1.4	1.2	1.1	1.0
E	2.5	1.7	1.2	0.9	b
F	b	b	b	b	b
Soil Profile Type	F_v For Shaking Intensity Levels				
	$A_V \leq 0.1$	$A_V = 0.2$	$A_V = 0.3$	$A_V = 0.4$	$A_V \geq 0.50^a$
A	0.8	0.8	0.8	0.8	0.8
B	1.0	1.0	1.0	1.0	1.0
C	1.7	1.6	1.5	1.4	1.3
D	2.4	2.0	1.8	1.6	1.5
E	3.5	3.2	2.8	2.4	b
F	b	b	b	b	b

Note: Use straight line interpolation for intermediate values of A_a and A_V

[a] Values for A_a, $A_V > 0.4$ are applicable to the provisions for seismically isolated and certain other structure

[b] Site specific geotechnical investigation and dynamic site response analyses shall be performed.

Empirical F_a and F_v Values

Adjusted NEHRP 94*			Empirical**	
$A_a = A_V$	F_a	F_V	F_a	F_V
0.1	1.3	1.5	1.1	1.5
0.2	1.2	1.4	1.0	1.4
0.3	1.1	1.3	0.9	1.4
0.4	1.1	1.2	0.9	1.4
0.5	1.1	1.2	0.8	1.4

*For site profile C + D relative to profile B + C

**Based on empirical attenuation relation (Abrahamson and Silva, 1997). F_a averaged from 0.1 - 0.5 sec, F_V averaged from 0.4 - 2.0 sec.

VERIFICATION OF RESPONSE SPECTRAL SHAPES

Code Category Profiles

To illustrate the type of shear-wave velocity profiles which are implied by the code categories (Table 1), median and ± 1 sigma profiles were developed for the UBC 94 and NEHRP 94 generic sites (Figure 1). For UBC 94 sites, as with the strong motion data, it was assumed that S_1 is comprised of NEHRP 94 B+C, S_2 is comprised of NEHRP 94 C+D, and S_3 is equivalent to NEHRP 94 E (Bill Joyner, personal communication). The generic profiles were produced from a profile database[2] of over 700 shear-wave velocity profiles using the criteria listed in Table 1. NEHRP 94 Site A, which represents very hard rock, is not currently represented in the profile database. The decrease in overall stiffness as well as variability is quite apparent in going from NEHRP 94 Sites B to E and from UBC 94 Sites S_1 to S_2.

NEHRP 94 Category E, soft sites containing significant amounts of soft to medium stiff clays soils, shows an increase in shear-wave velocity near the surface (Figure 1). This is likely due to artificial fill at sites located near the edges of San Francisco Bay and is a common occurrence at soft sites in the built environment.

The apparent decrease in variability as stiffness decreases represents a potentially important feature in the category profiles shown in Figure 1. This trend suggests that the variability in strong ground motions could also be dependent on site stiffness. As a result, higher ground motion variability might be expected at NEHRP 94 Category B sites compared to NEHRP 94

---

[2]Pacific Engineering profile database

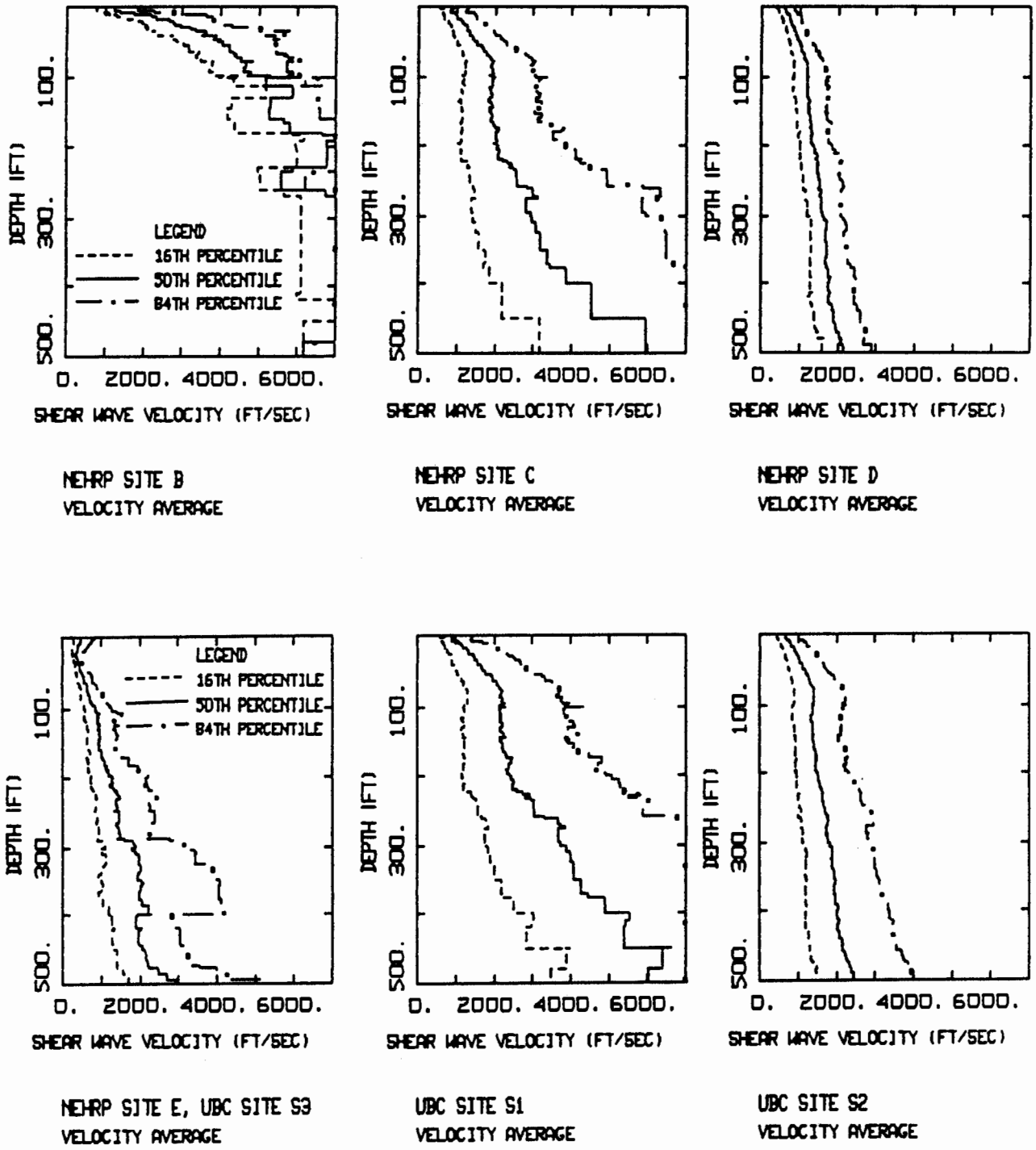

Figure 1. Representative median and $\pm$ 1 sigma shear-wave velocity profiles for the NEHRP 94 provisions and UBC 94 site classes (Table 1) (NEHRP 94 site class A, very hard rock, is currently not represented in the profile database).

Category D for example. This site category dependent variability may result in a non uniform degree of conservatism in the code spectral shapes if this effect is not explicitly addressed. Future revisions of the code shapes should examine the possible site category dependent variability with detailed statistical analyses and, if warranted, accommodate its effects to achieve overall risk consistency in the design shapes.

Strong Motion Database

The strong motion database available for development of statistical 5% damped response spectral shapes was compiled by Pacific Engineering and Analysis and contains approximately 100 earthquakes in the magnitude range of about **M** 5 to **M** 7.4. The database consists of over 2,000 recordings and most of the available Volume 1 records have been reprocessed to extend both the short and long period portions of the motions. Recording sites have been assigned available USGS site codes (Boore et al., 1994). Sites which did not have assigned codes but which had available shear-wave velocity profiles were classified according to the criterion listed in Table 1. Records were assigned UBC 94 site categories based on the following assumption: S_1 = NEHRP 94 B+C, S_2 = NEHRP 94 C+D, and S_3 = NEHRP 94 E.

For applications to code shapes, the magnitude selection was limited to **M** 6.3 and above. The breakdown in mean magnitudes, distances, and PGA's for each site category is shown in Table 3. Also shown in Table 3 are the number of records (spectra) and earthquakes contributing to each site category. The statistical shapes are computed by normalizing each record by its peak acceleration and averaging assuming a lognormal distribution. Records are weighted such that each earthquake within a site category receives equal weight. This assures

that the statistical shapes actually reflect a shape appropriate for the mean magnitude of each bin. Interestingly, giving each record equal weight results in very similar shapes. Excluding the near-fault 0-10 km shapes, the average magnitude is 6.75 at a distance range of about 35 to 40 km and with a mean PGA value of approximately 0.15g.

Table 3
MEAN MAGNITUDES AND DISTANCES FOR THE RESPONSE SPECTRAL SHAPES

Site	Number of Records	Number of earthquakes	$\overline{M}$	$\overline{D}$	$\overline{PGA}$ (g)
S_1	164	10	6.88	34	0.16
S_2	340	13	6.75	32	0.18
S_3*	126	10	6.75	42	0.12
$S_1(10)$**	20	6	6.91	5	0.62
$S_2(10)$**	46	5	6.62	5	0.42
B	42	6	6.94	39	0.15
C	120 (14)***	8 (4)***	6.86 (6.82)***	33 (13.1)***	0.17 (0.29)***
D	218 (20)***	10 (4)***	6.69 (6.75)***	32 (13.1)***	0.18 (0.37)***
E*	126 (110)***	10 (6)***	6.75 (6.80)***	42 (45)***	0.12

*SMART 1 array at Lotung classified as E.
**Data restricted to closest fault rupture distance $\leq$ 10 km.
***Data contained in expected rock PGA bins (Figure 3)

UBC 94 Shapes

Figures 2a to 2c shows the statistical shapes (computed from recordings) compared to the code requirements for UBC 94 sites S_1, S_2, and S_3 (too few data were available for site S_4) and Table 3 shows the data distributions in M, distance, and number of records. The UBC 94 spectral shape requirements are shown for both the equivalent-lateral force (ELF) and dynamic-analysis design procedures. The spectral shape for ELF design is given by the expression

$$\frac{S_a(T)}{Z}=\min\left[2.75,\ \frac{1.25S}{T^{2/3}}\right] \qquad (1)$$

where S is the soil factor given in Table 1 and Z is the zone factor representing design peak acceleration. The first term in brackets controls short periods and the second term controls longer periods. The unbiased static provisions, which use a spectral decay of T^{-1} instead of $T^{-2/3}$ are also shown. The spectral shape for dynamic analysis is given only in graphical form in the code, but is well approximated by the expression

$$\frac{S_a(T)}{Z}=\min\left[1+aT,\ 2.5,\ \frac{1.05\,S'}{T}\right] \qquad (2)$$

where a is 10 for S_1 and S_2 soils and is 7.5 for S_3 soils (dynamic analysis of buildings on S_4 soils require site-specific investigations), S' is a soil factor given in Table 1. This shape is close to the unbiased shape at long periods and saturates to PGA at short periods. The statistical shapes for S_1 and S_2 are similar, with the S_1 shape peaking at a slightly shorter period than the S_2 shape possibly reflecting stiffer site conditions. The similarity in shapes is possibly due to the assumed definition of S_1 and S_2 being overlapping combinations of NEHRP 94 sites B, C, and D. This points out a possible disadvantage of the NEHRP 94 classification scheme in not considering profile depth as part of the classification criterion. Since profile information rapidly decreases at depths beyond about 70-100 ft, it is very difficult to accurately segregate profiles into depth bins. In general, for magnitude of about 6.75, the UBC 94 shapes are consistent with the ground motion spectral shapes and exceed the median statistical shapes from 0.1 to 10.0 sec.

To assess near-fault effects, statistical spectra for site categories S_1 and S_2 were developed for sites at fault rupture distances of 0 to 10 km (no S_3 or S_4 sites were available). These results

are shown in Figures 2d and 2e and suggest that the code shapes (particularly the lateral force requirements) do reasonably well on average for M in the range of about 6.6 to 6.9 (Table 3). However, the S_1 dynamic analysis shape is close to the median ground motion at very short periods (< 0.08 sec) and both the S_1 and S_2 dynamic shapes are close to the median ground motion near one second.

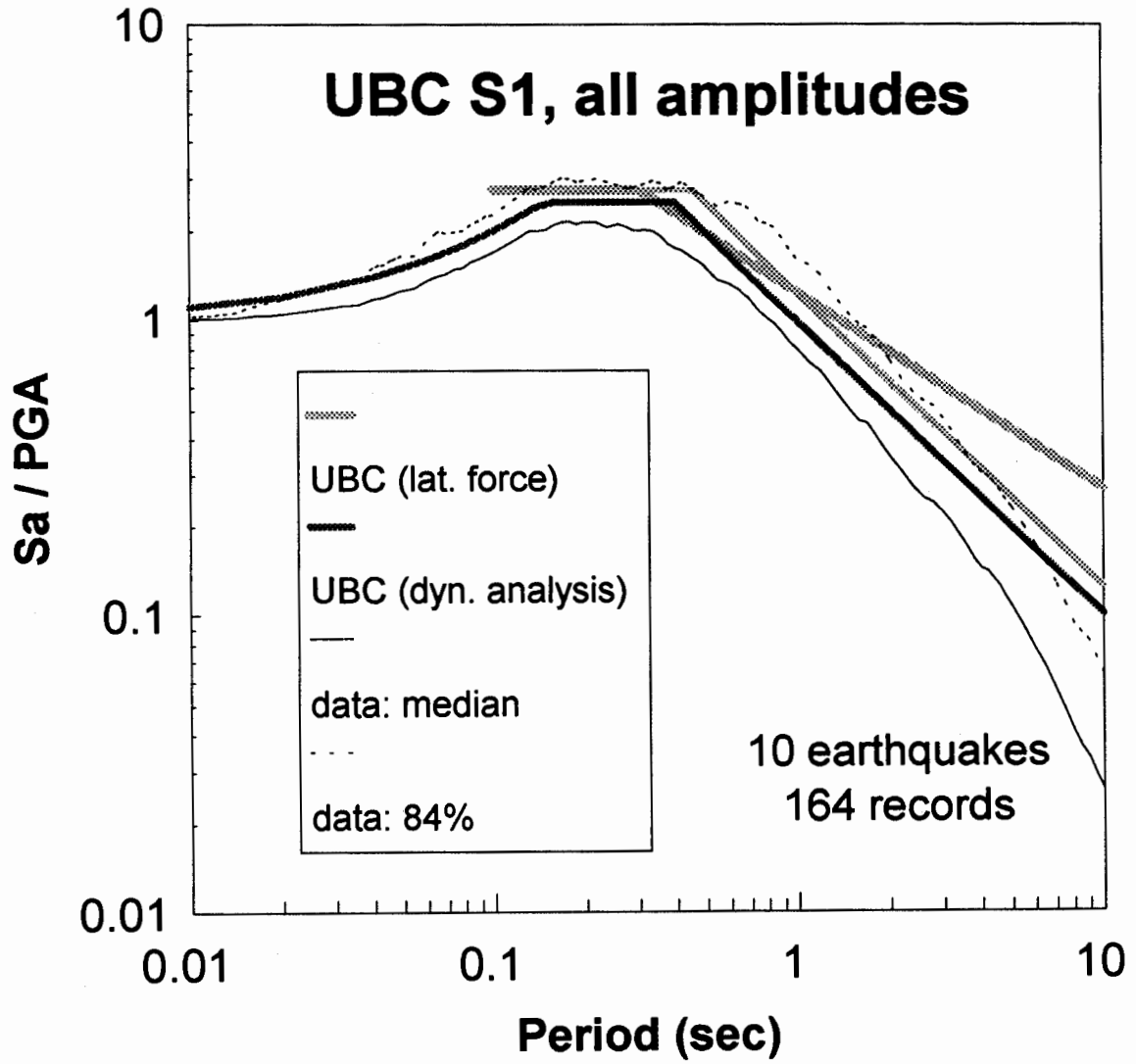

Figure 2a. Comparison of UBC 94 code shapes with statistical spectra ($\overline{M}$ = 6.88, Table 3) computed from data recorded at sites classified as S_1 (Table 1).

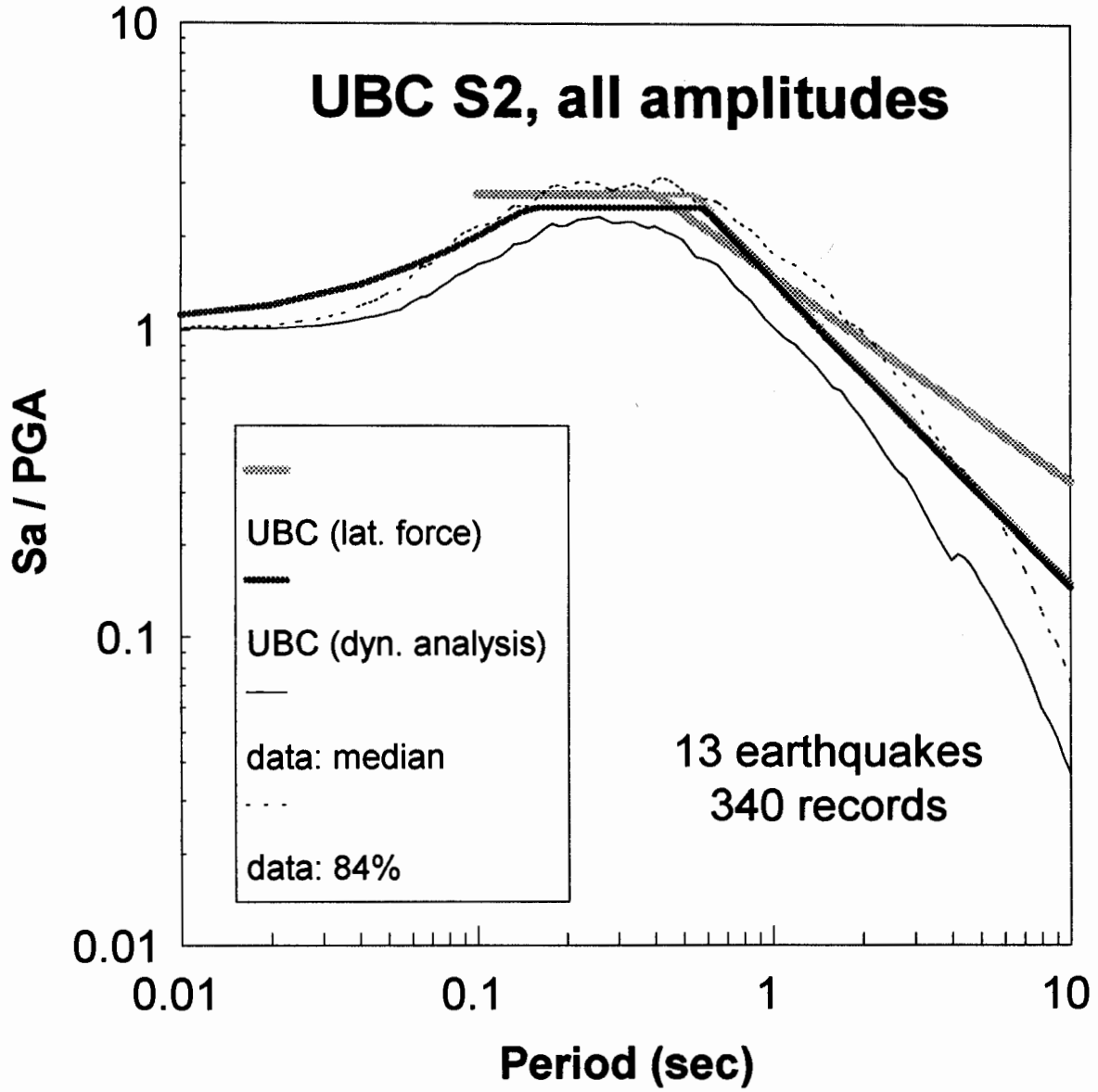

Figure 2b. Comparison of UBC 94 code shapes with statistical spectra ($\overline{M}$ = 6.75, Table 3) computed from data recorded at sites classified as S_2 (Table 1).

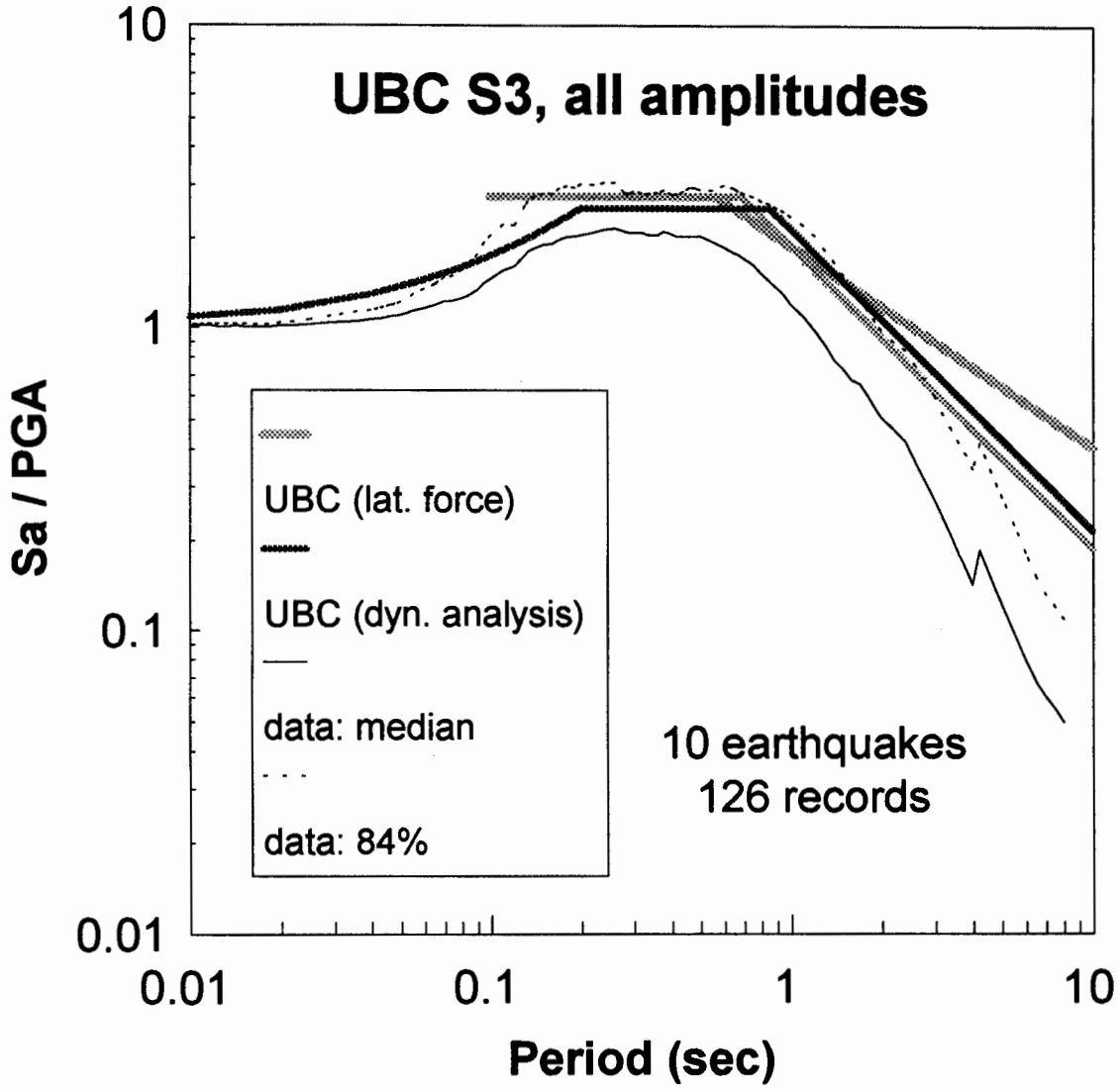

Figure 2c. Comparison of UBC 94 code shapes with statistical spectra ($\overline{M}$ = 6.75, Table 3) computed from data recorded at sites classified as S_3 (Table 1).

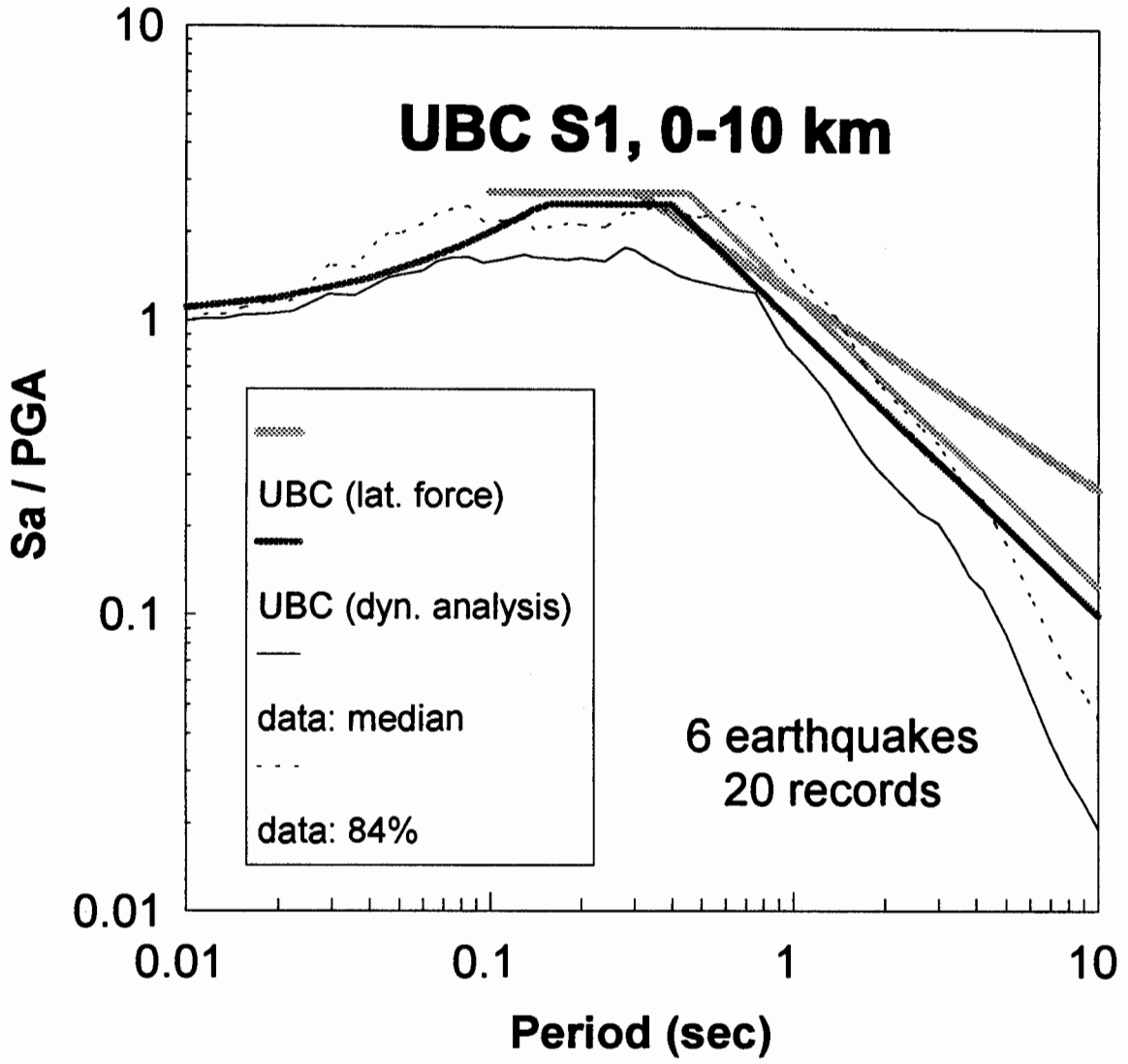

Figure 2d. Comparison of UBC 94 code shapes with statistical spectra ($\overline{M}$ = 6.91, Table 3) computed from data recorded at sites classified as S_1 (Table 1) at fault rupture distances from 0 to 10 km.

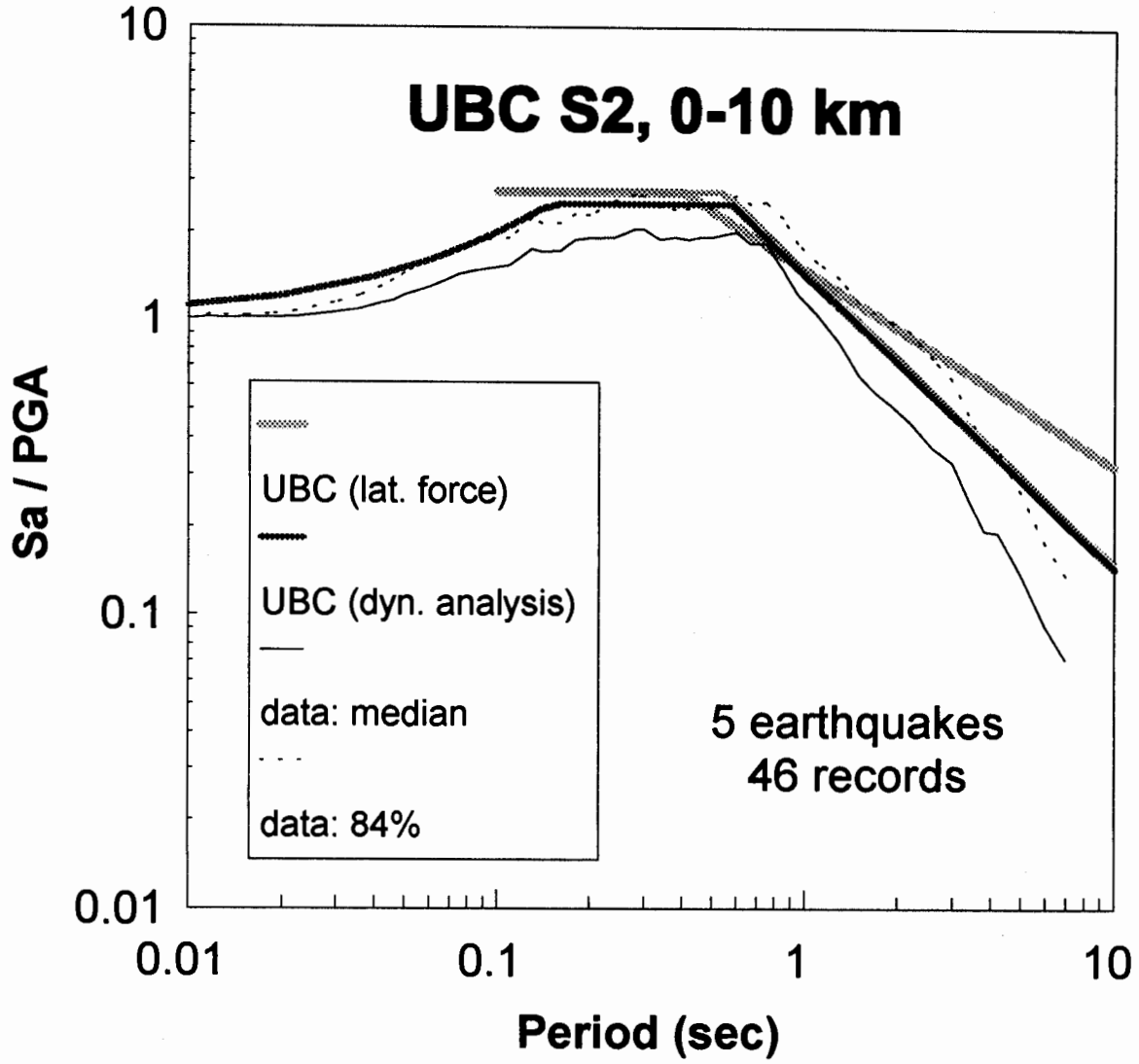

Figure 2e. Comparison of UBC 94 code shapes with statistical spectra ($\overline{M}$ = 6.62, Table 3) computed from data recorded at sites classified as S_2 (Table 1) at fault rupture distances from 0 to 10 km. Site categories S_3 and S_4 have too few data over this distance range to provide stable statistical spectra.

NEHRP 94 Shapes

The comparisons of the statistical spectra for NEHRP 94 sites B, C, D, and E to the code provision design shapes are shown in Figures 3a to 3f. For the code shapes, both the provision requirements, which accommodate structural considerations, and the unbiased spectra are shown. Site A, very hard rock, is not shown as there are currently no sites in the database assigned this category.

The NEHRP 94 spectrum is given by the expression:

$$Sa(T)=\min\left[(1+5T)F_aA_a,\ 2.5F_aA_a,\ \frac{1.2F_vA_v}{T^{2/3}},\ \frac{3F_vA_v}{T^{4/3}}\right] \qquad (3)$$

and the unbiased shape is obtained by changing 1.2 to 1.0, $T^{2/3}$ to T, and 3 to 1.9 in the above equation. The first two terms in brackets control short periods (shorter than approximately 0.5 sec. The first term applies only to site categories D, E, or F, and only to dynamic analysis and modes other than the first, and the third term controls periods of approximately 0.5 to 4 seconds. The first important difference with the UBC 94 spectrum is the use of two anchoring or controlling ground-motion amplitudes. The short-period portion is anchored to F_a times A_a, where A_a is equivalent to the UBC 94 zone factor Z. The intermediate and long-period portion is anchored to F_a times A_v, where A_v is related to peak ground velocity and is roughly equivalent to spectral acceleration at 1 sec for 5% damping. This concept dates back to the Newmark-Hall (CR-0098) shapes where portions of the design spectra were approximated as two straight lines (in log-log space) with amplitudes proportional to peak ground acceleration and velocity. The second important difference is the presence of two site coefficients F_a and F_v for the short- and long-period portions of the spectrum. The third difference is the treatment of nonlinear site

response by means of F_a and F_v values that depend on the rock ground-motion amplitudes A_a and A_v, respectively (see Table 2).

To compare statistical shapes to the NEHRP 94 design spectral shapes for each category, it was assumed that $A_a = A_V$, which is the case for much of California in the current NEHRP 94 maps (Table 4). In addition, because the shapes depend upon rock motion amplitude (A_a and A_V) through the F_a and F_v factors (Table 2), the data were separated into distance bins based on expected rock PGA (A_a) ranges. The expected rock PGA values were computed from a recently developed empirical attenuation relation which classifies rock as NEHRP 94 sites B plus C (Abrahamson and Silva, 1997). In the comparisons shown in Figure 3a, site B statistical shapes represents all distances ($M > 6.3$) since F_a and F_v are 1 for all A_a and A_V. The mean magnitude is near M 6.9 with mean distance and PGA of 40 km and 0.15g respectively (Table 3). For sites C, D and E (Figures 3b to 3d) the highest rock PGA (A_a) ranges are shown which have sufficient data to constrain shapes ($\geq$ 4 earthquakes and $\geq$ 15 spectra). The C and D sites reflect records selected from distance ranges where the expected rock PGA ranges from about 0.25 to 0.35g for $M \geq 6.3$. For these cases A_a is taken as 0.20g ($A_V = 0.2$g) to construct the NEHRP 94 shapes. Mean magnitudes for sites C and D are 6.86 and 6.62 respectively (Table 3). For site E, to provide enough data for stable statistical shapes, the expected rock PGA range combines the two lowest A_a and A_V bins, 0.1 and 0.2g and the expected rock PGA range used was 0.0 to 0.25g. The mean magnitude for the soil spectra is 6.75.

For sites B and C (Figures 3a and 3b) the code provision shape exceeds the median statistical shape over the range of 0.1 to 10.0 sec. For site D (Figure 3c), the code provision

exceeds the statistical shape at long to intermediate periods ($\geq$ 0.3 sec) but is below the data at short periods ($<$ 0.3 sec). For site E (Figure 3d), the code provision exceeds the statistical shape but the margin is small at short periods ($\leq$ 0.5 sec).

To assess very high amplitude long period motions, Figure 3e compares the NEHRP 94 B shape to the two horizontal components of the Lucerne site from the M 7.3 1992 Landers earthquake (Professor W. Iwan, personal communication). The site is at a fault distance of 1.1 km and has very high motions on the 260° component (fault normal). Interestingly the code provision shape does extremely well from 0.1 to 10.0 sec. However, it must be emphasized that, since the average recorded PGA at the site is about 0.8g, scaling the NEHRP 94 shape to an A_a = 0.4g would result in the long period absolute level of the 260° component exceeding the code provision by a factor of about 1.5. These results are shown in Figure 3f and indicate the code provision in absolute level would be close to the average horizontal component at long periods.

As an additional evaluation of the NEHRP 94 provisions, the nonlinear F_a and F_v factors were estimated using the empirical attenuation relation of Abrahamson and Silva (1997). In this relation, both rock and soil sites are considered with rock generally reflecting NEHRP 94 B and C (hard rock to very stiff soil) and soil NEHRP 94 C and D (stiff soils). To accommodate this classification, the NEHRP 94 factors (F_a and F_v) were adjusted to reflect ratios of site C + D to site B + C. The empirical F_a and F_v factors were computed as ratios (soil/rock) of empirical response spectra, averaged 0.1 to 0.5 sec for F_a and 0.4 to 2.0 sec for F_v, for increasing rock PGA values. The results are shown in Table 2 and reflect comparable values for the adjusted

NEHRP 94 factors and empirical factors. The empirical F_a are lower (20 to 40%) and show a stronger nonlinear effect than the code provision. For F_v, the empirical factors show little nonlinear effects while the NEHRP 94 F_v factors reflect about the same nonlinearity as the NEHRP 94 F_a factors. Crouse and McGuire (1996), who developed empirical F_a and F_v factors from recordings of strong ground motions (prior to the Northridge and Kobe earthquakes), also found differences in the degree of nonlinearity in the code provision factors and the empirically derived factors. While their results are not directly comparable to ours, since our results reflect adjusted factors, both studies suggest the possibility of an inappropriate degree of nonlinearity in the current F_a and F_v factors and further work is warranted in resolving this issue.

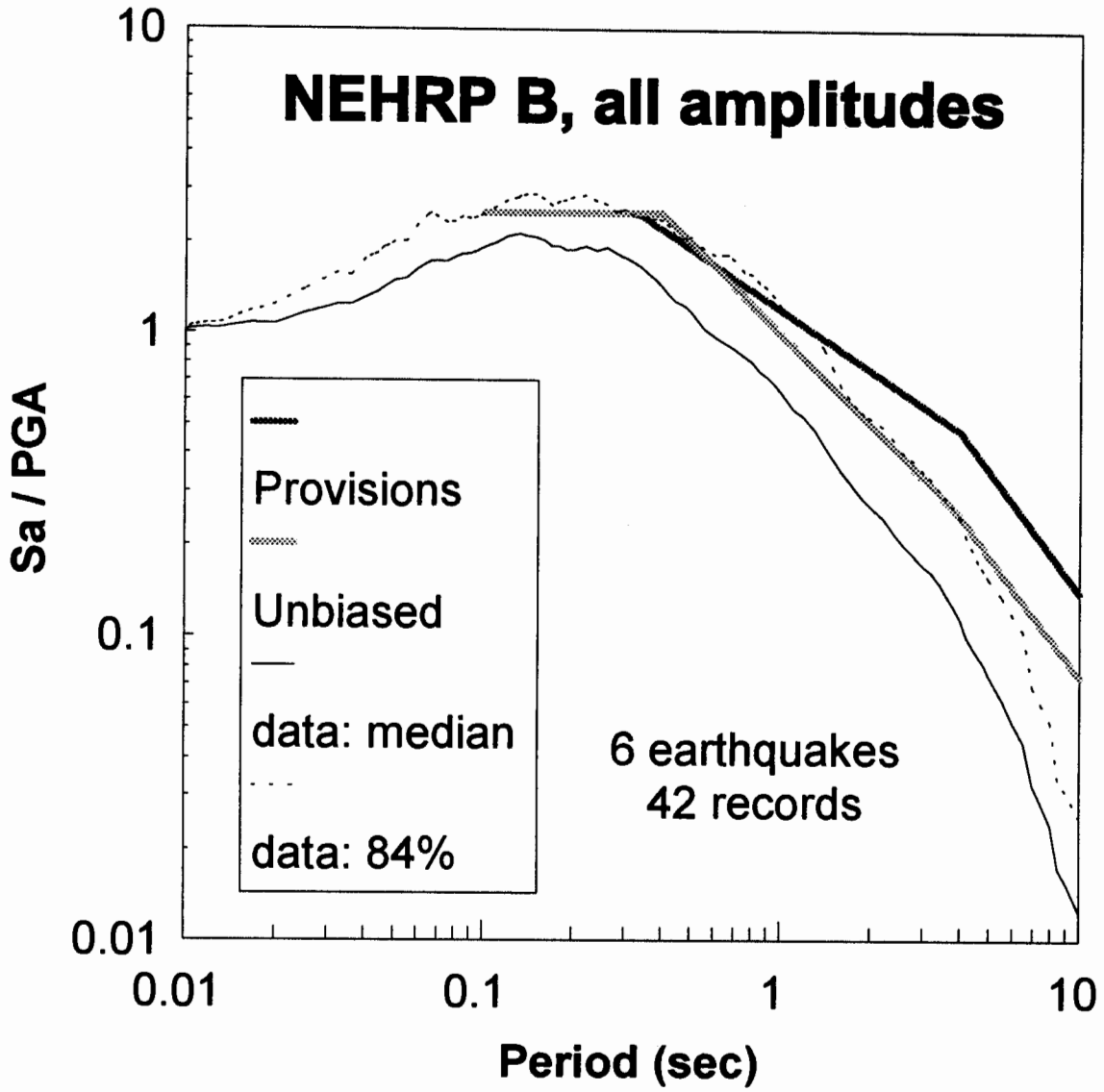

Figure 3a. Comparison of NEHRP 94 code provision shapes with statistical spectral shapes ($\overline{M}$ = 6.94, Table 3) computed from data recorded at sites classified as NEHRP 94 B (Table 1). For site B, since the F_a and F_v values are independent of level of motion (A_a and A_v, Table 2), all the site B data (Table 3) were used to construct the statistical shapes.

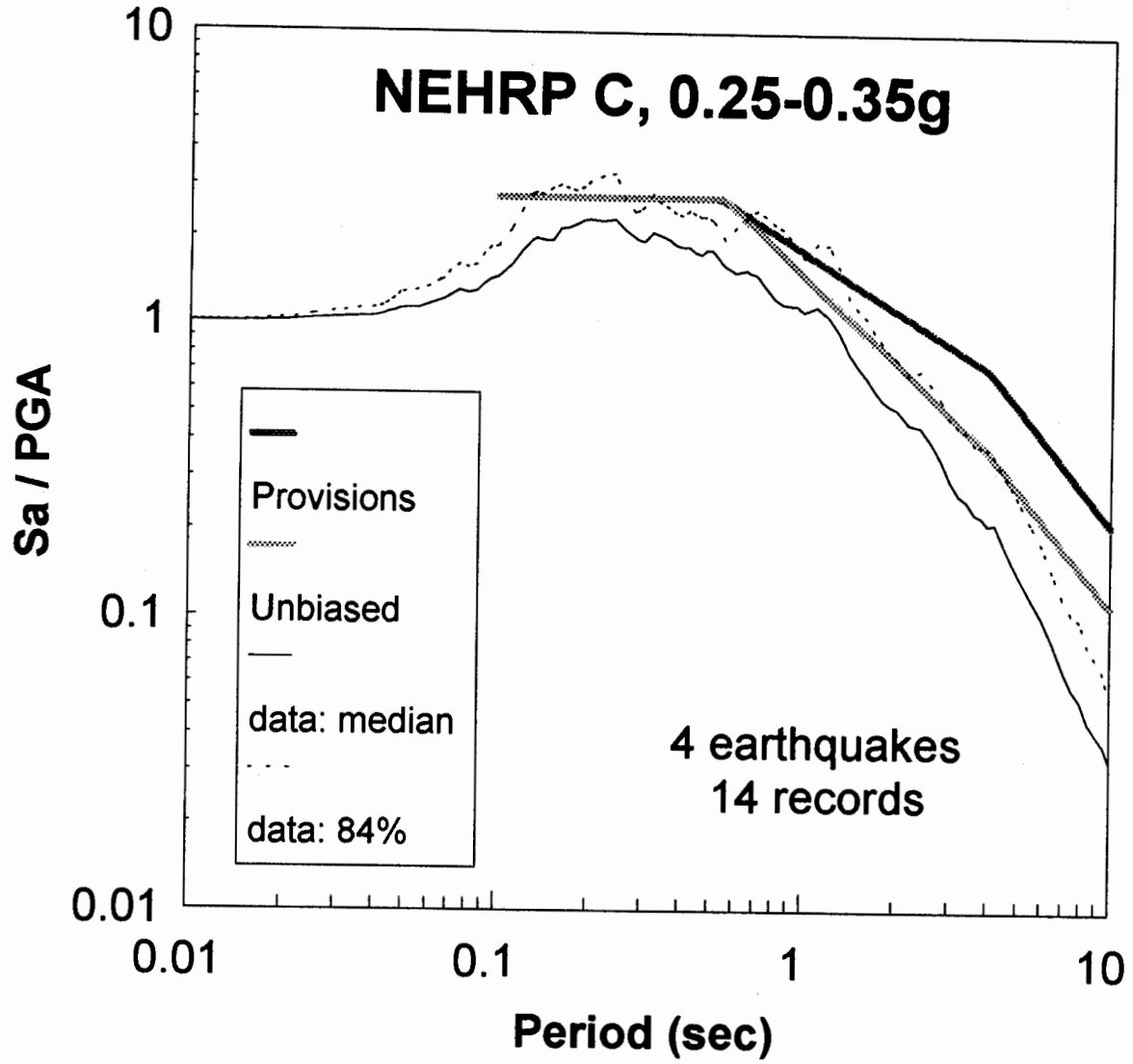

Figure 3b. Comparison of NEHRP 94 code provision shapes with statistical spectral shapes ($\overline{M}$ = 6.86, Table 3) computed from data recorded at sites classified as NEHRP 94 C (Table 1). Site C data are restricted to distance ranges where the expected rock peak accelerations range from 0.25g to 0.35g.

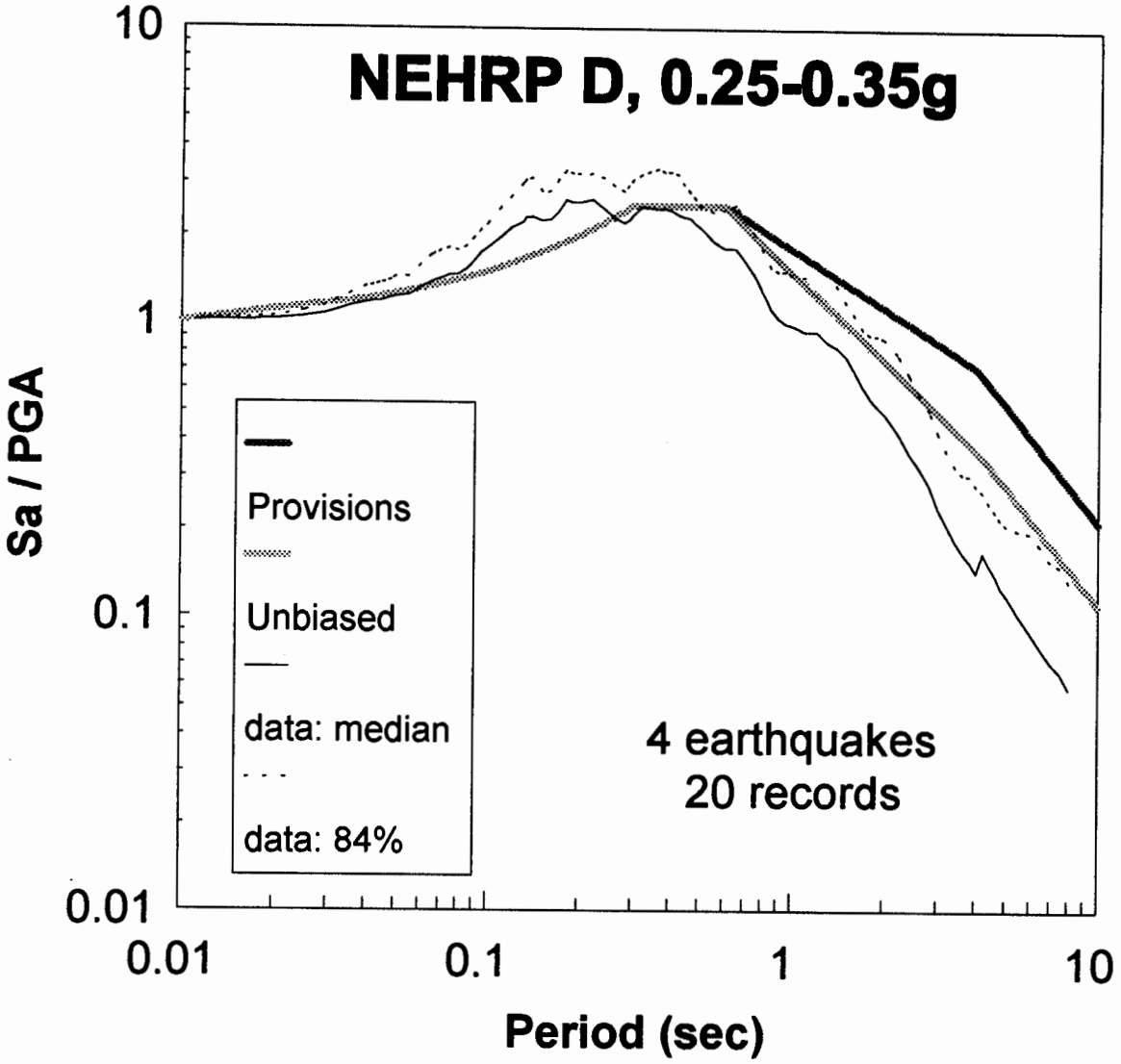

Figure 3c. Comparison of NEHRP 94 code provision shapes with statistical spectral shapes ($\overline{M}$ = 6.69, Table 3) computed from data recorded at sites classified as NEHRP 94 D (Table 1). Site D data are restricted to distance ranges where the expected rock peak accelerations range from 0.25g to 0.35g.

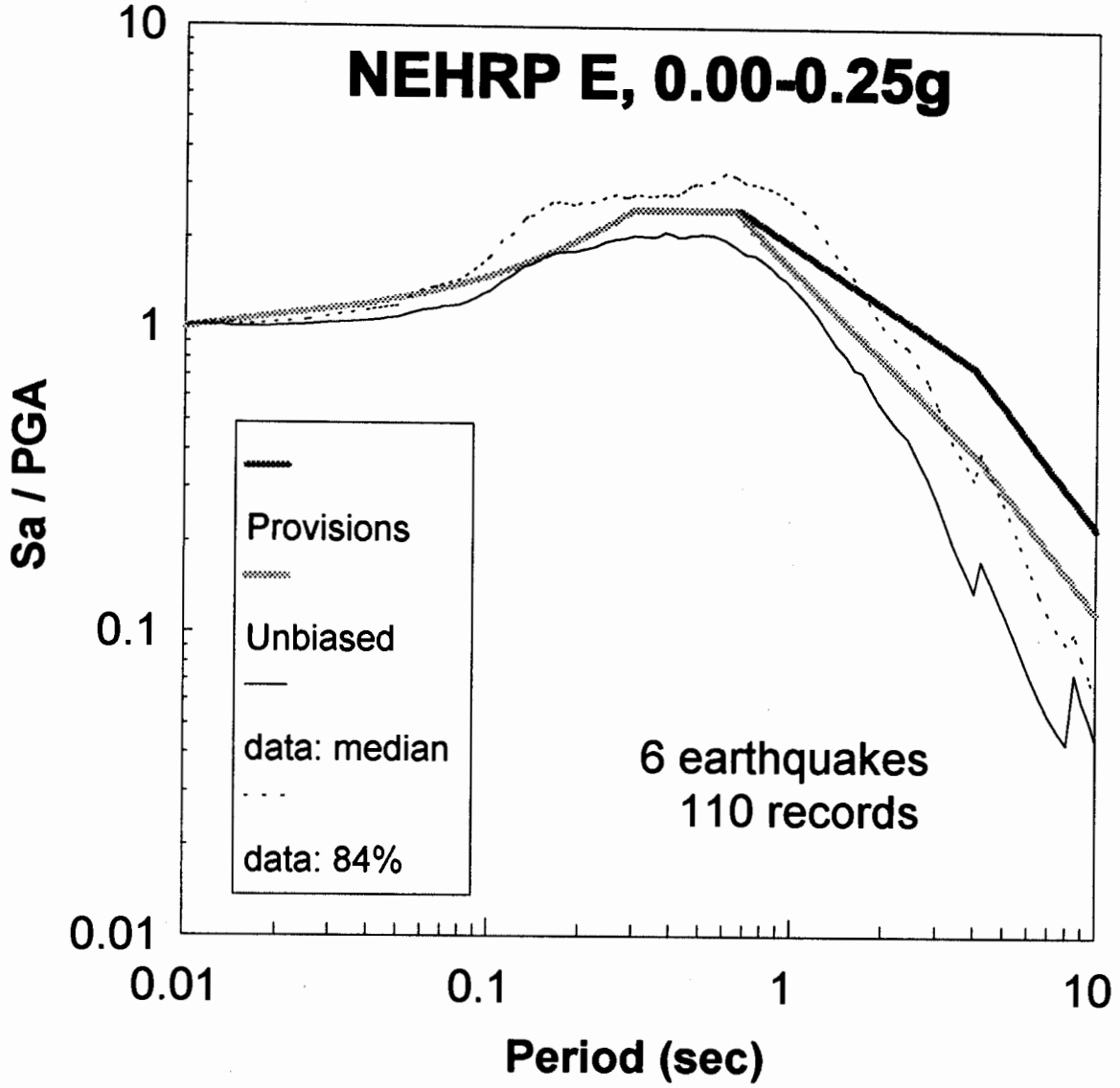

Figure 3d. Comparison of NEHRP 94 code provision shapes with statistical spectral shapes ($\overline{M}$ = 6.75, Table 3) computed from data recorded at sites classified as NEHRP 94 E (Table 1). Site E data are restricted to distance ranges where the expected rock peak accelerations range from 0.01g to 0.25g.

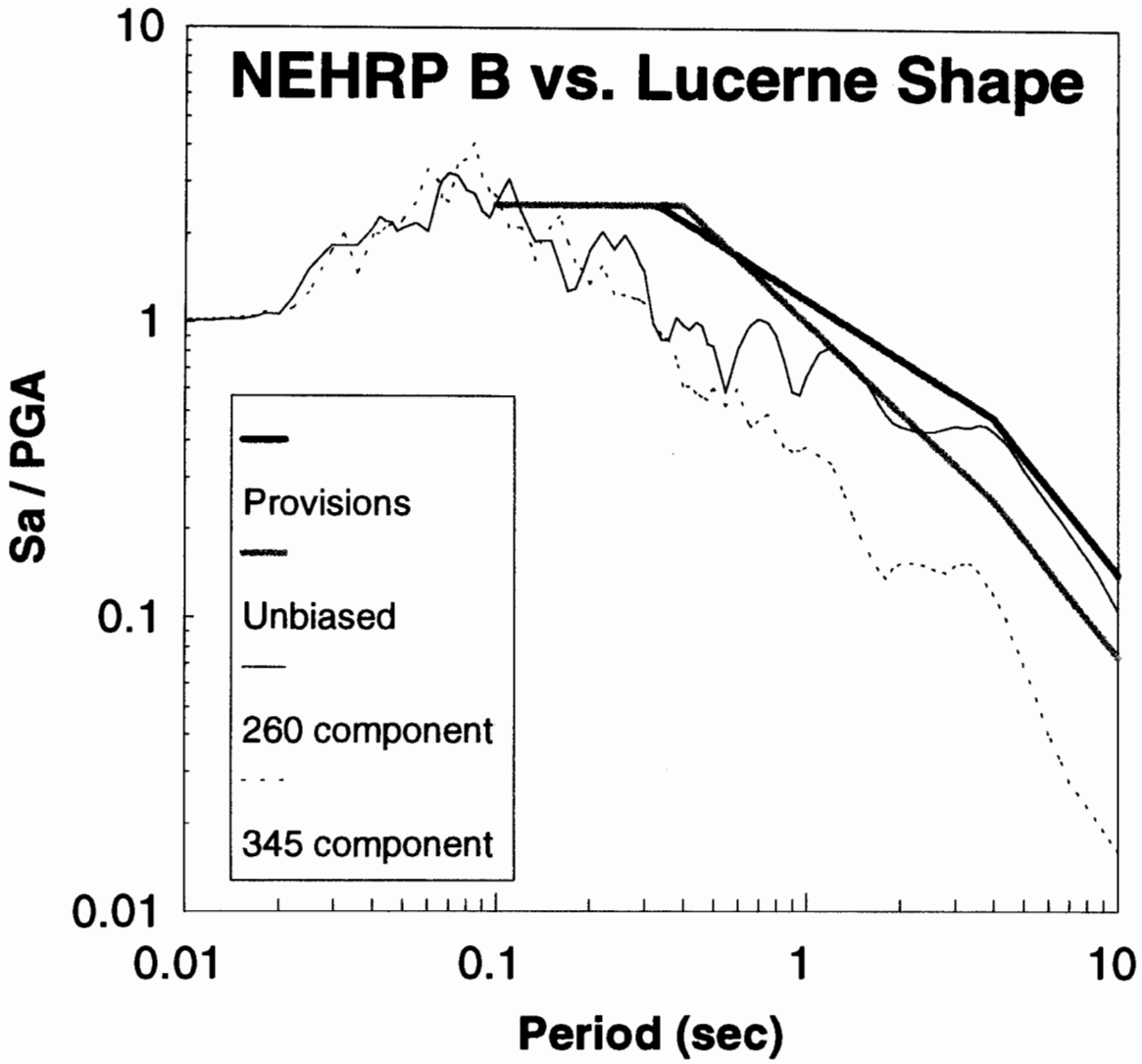

Figure 3e. Comparison of NEHRP 94 provision code shapes with the Lucerne (Southern Cal. Edison) site records (shapes) for the M 7.3 1992 Landers earthquake to the NEHRP 94 site B shape. The site is at a fault distance of about 1.1 km and consists of shallow soil (about 20 ft) over hard California rock.

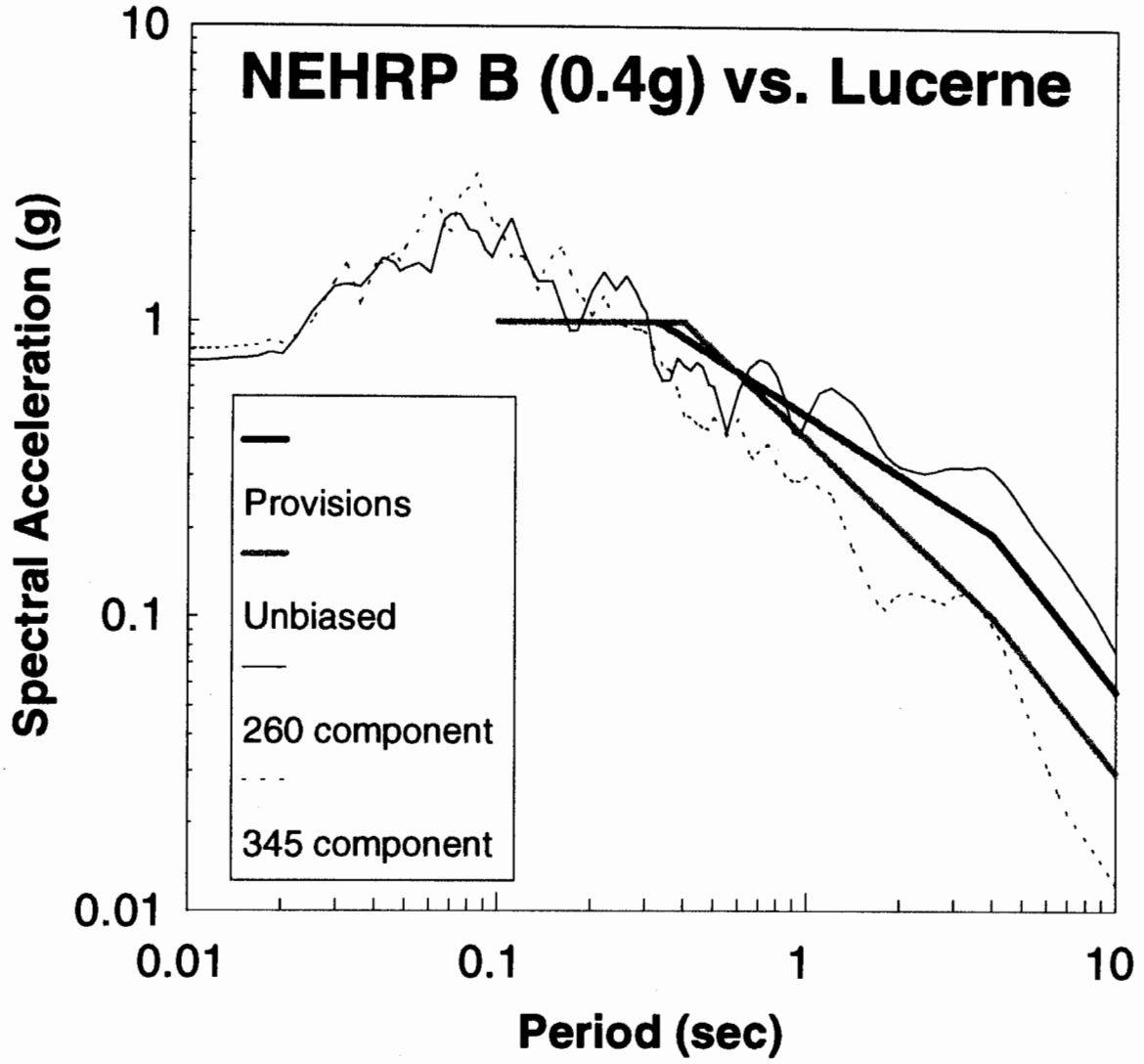

Figure 3f. Comparison of NEHRP 94 provision code spectra using A_a = 0.4g with the Lucerne (Southern Cal. Edison) site records for the M 7.3 1992 Landers earthquake to the NEHRP 94 site B shape. The site is at a fault distance of about 1.1 km and consists of shallow soil (about 20 ft) over hard California rock. The average recorded peak accelerations for the horizontal components is about 0.8g.

PROBABILISTIC SEISMIC HAZARD RESULTS FOR SELECTED CITIES AND COMPARISONS TO CODE SPECTRA

The purpose of these calculations and the comparisons that follow is to investigate the consistency of the UBC 94 and NEHRP 94 code spectral shapes with the uniform-hazard spectra (UHS) calculated by probabilistic seismic-hazard analysis (PSHA). In particular, we wish to determine to what extent it is necessary to have two spectral anchor points (as in the NEHRP 94 code), in order to accommodate differences in the shape of the UHS that arise from differences in the nature of the seismic threat at different California cities. For instance, one anticipates that the design spectrum for San Francisco should have more low-frequency energy than the one for Los Angeles because more of the hazard at San Francisco comes from large earthquakes in the San Andreas fault. In addition, we wish to investigate the effect of larger uncertainty in the attenuation functions for long periods, which tends to flatten the UHS at these periods. The interest here is more on the shape of the UHS, rather than on the absolute amplitudes of the code shapes anchor points.

The source characterizations used for the probabilistic seismic hazard calculations (source geometries, magnitude-recurrence models, maximum magnitude, and their corresponding uncertainties) come from recent published studies performed by others. The source characterization for Los Angeles come from Petersen et al. (1995) and that for San Francisco from Youngs et al. (1994). The source characterization for Sacramento is a combination of the Youngs et al. characterization and USGS sources for the Sacramento region and the Sierra Nevada (Hansen and Perkins, 1995). Some minor modifications were introduced in these source

characterizations, for the sake of simplicity.

The following three attenuation equations for soil were considered: Abrahamson and Silva (1997), Boore et al. (1994), and Sadigh (1988). These attenuation equations apply to UBC 94 soil category S_2 and to a mixture of NEHRP 94 soil categories C and D (with a majority of D). These three attenuation equations reflect recent strong-motion data from California and include the effect of fault type (thrust or strike-slip). The Abrahamson and Silva equations also predict different amplitudes for the up-thrown and down-thrown blocks of a thrust fault, but this effect was not considered in the calculations. These two effects are important only for Los Angeles area.

PSHA calculations at the three cities are performed for peak ground acceleration (PGA) and for spectral accelerations (S_a) at 0.04, 0.1, 0.2, 0.4, 1, 2, and 4 sec (5% damping). These results are used to construct mean UHSs for 90% non-exceedence probability in 50 years. This exceedence probability (equivalent to an annual exceedence probability of 2.1×10^{-3} or a return period of 475 years) is the one implied in both the UBC 94 and NEHRP 94 codes. In addition, we determine the design earthquakes associated with these hazard results, for both PGA and S_a(1 sec), using McGuire's (1995) procedure. A design earthquake is defined in terms of a magnitude, a distance, and an attenuation-equation ϵ (number of standard deviations above the median). Results from the PSHA calculations are shown in Table 4, which also shows the ground-motion amplitudes in the UBC 94 and NEHRP 94 codes, as well as the interim USGS values (Frankel et al., 1995).

Table 4
HAZARD-ANALYSIS RESULTS AND CODE ACCELERATION VALUES

City	UBC 94 Z(g)	NEHRP 94 A_a(g) A_v(g)	USGS Interim hazard maps[1,2] PGA(g)	Probabilistic Seismic Hazard Analysis[1] (UBC S_2, NEHRP C-D soil)	
				PGA(g) S_a(1Hz)(g)	Design Earthquake
Los Angeles[3]	0.4	0.4 0.4	0.5	0.45 0.55	M 5.9 at 9 km, ϵ=1.5 M 6.5 at 10 km, ϵ=0.9
San Francisco[4]	0.4	0.4 0.4	0.7	0.44 0.73	M 7.7 at 14 km, ϵ=0.60 M 7.7 at 14 km, ϵ=0.35
Sacramento[3]	0.3	0.2 0.3	0.12	0.15 0.22	M 5.1 at 15 km, ϵ=1.0 M 7.8 at 130 km, ϵ=1.0

[1] Associated with a mean non-exceedence probability of 90% in 50 years.
[2] UBC 94 S_1, NEHRP 94 B site conditions. Values shown are approximate due to the difficulty in reading these values from large-scale maps.
[3] Downtown
[4] Financial District

The magnitudes and distances that control seismic hazard at these three cities are quite different, as illustrated by the design earthquakes given in Table 4. This is confirmed by Figures 4a to 4c, which show the contributions of the various magnitudes, distances, and attenuation ϵs to the mean hazard for PGA and S_a (1 Hz) for Los Angeles, San Francisco, and Sacramento respectively. Local faults (Hollywood, Elysian Park, and others) dominate the hazard in Los Angeles while the San Andreas fault dominates the hazard in San Francisco, as well as the 1 Hz hazard in Sacramento. The local area source dominates the PGA hazard in Sacramento. These differences have an effect on spectral shapes, as will be shown below.

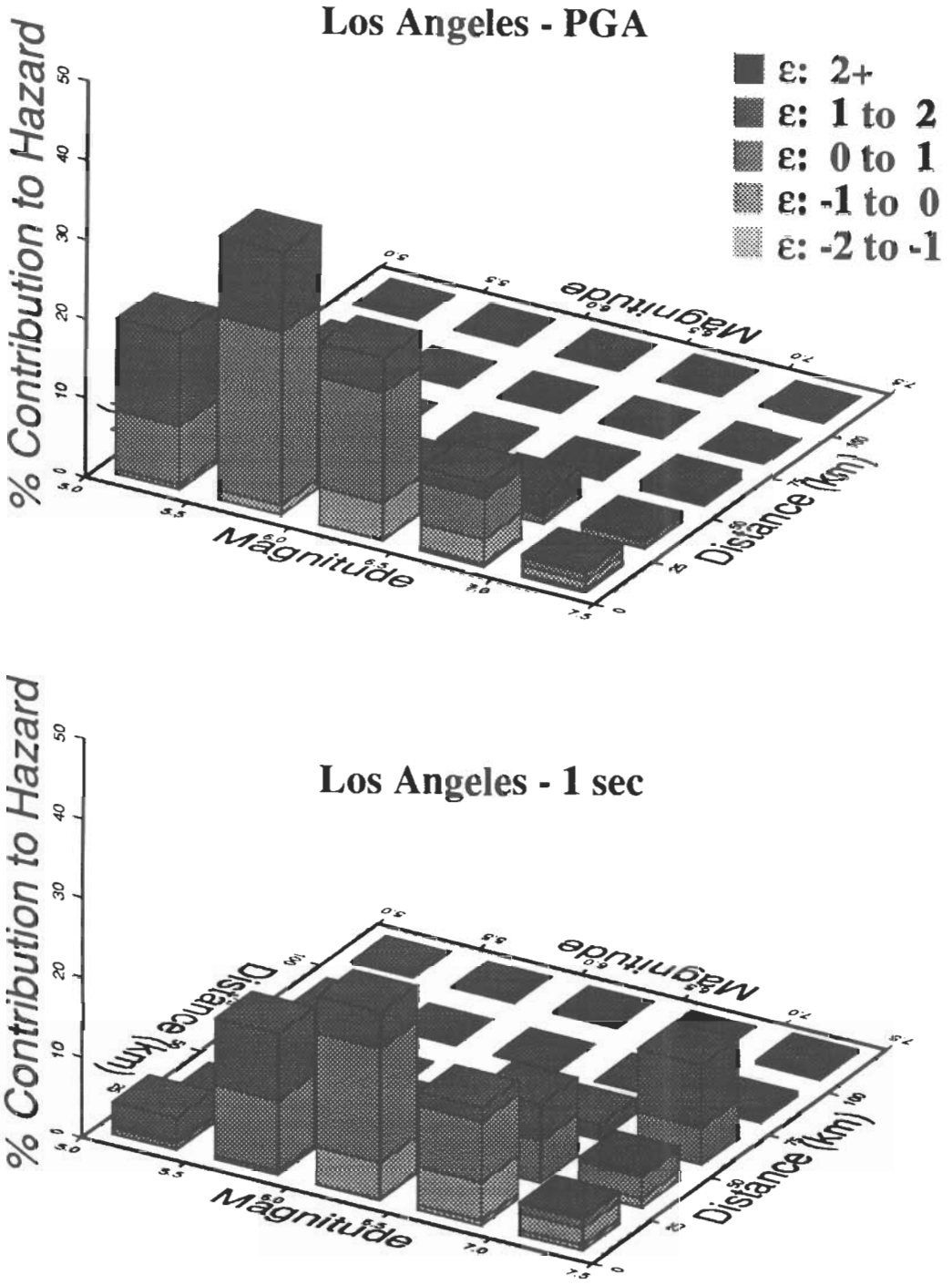

Figure 4a. De-aggregation of the mean exceedence probability by magnitude, distance, and ground-motion ϵ for Los Angeles. Non-exceedence probability: 90% in 50 years.

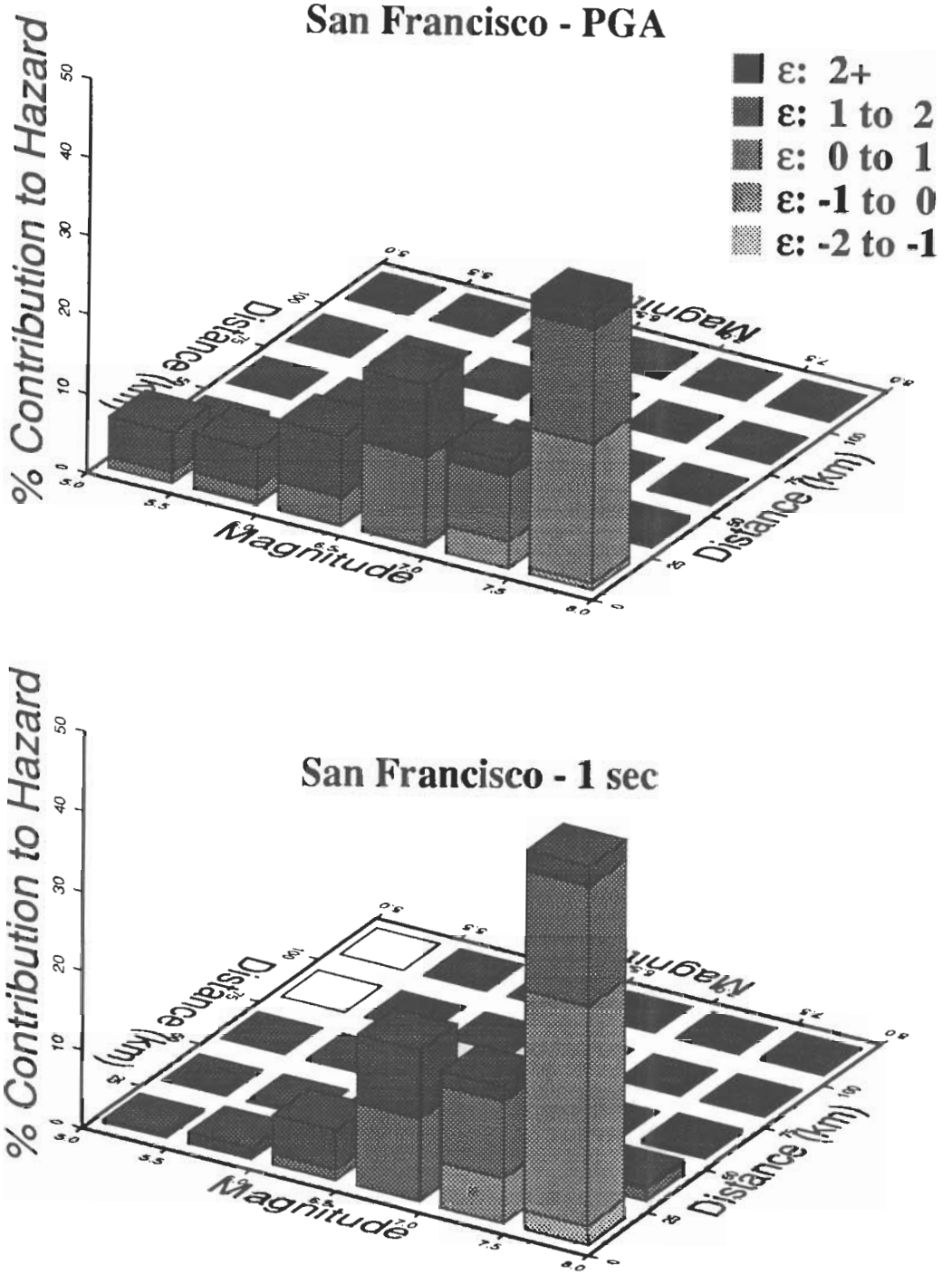

Figure 4b. De-aggregation of the mean exceedence probability by magnitude, distance, and ground-motion ϵ for San Francisco. Non-exceedence probability: 90% in 50 years.

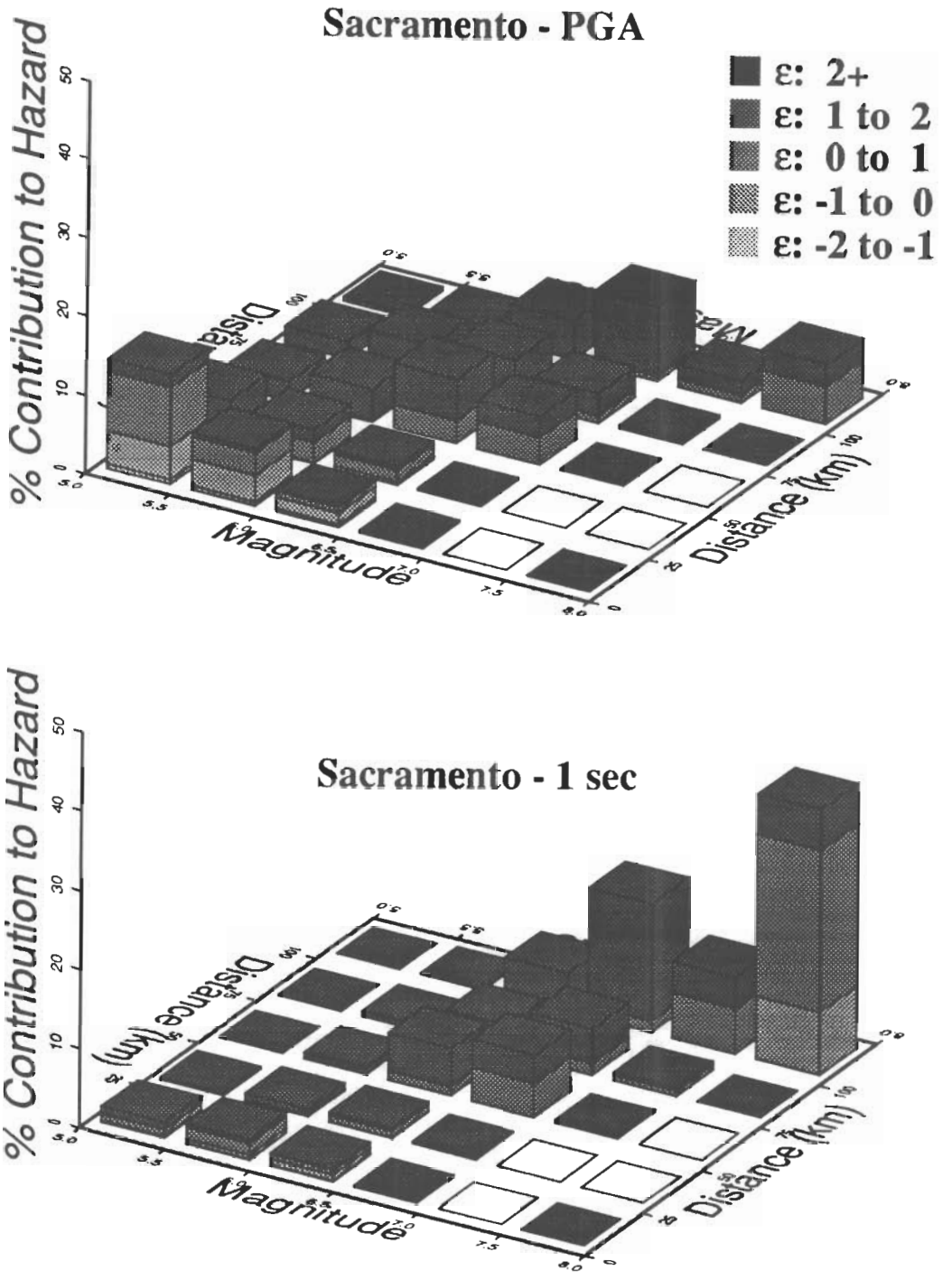

Figure 4c. De-aggregation of the mean exceedence probability by magnitude, distance, and ground-motion ϵ for Sacramento. Non-exceedence probability: 90% in 50 years.

If one uses the non-Poissonian recurrence models and parameters adopted by the Working Group on California Earthquake Probabilities (1990), one finds that the importance of the San Andreas fault is greatly reduced (J. Marrone, personal communication). This is likely due to the low coefficients of variation of recurrence times used in that study (0.21), which are now considered too low (see Working Group on California Earthquake Probabilities, 1995). More realistic values of the coefficient of variation (e.g, 0.5) are expected to yield results similar to those presented here.

It is also important to note that the results for San Francisco were obtained for a site in the Financial District and are not necessarily applicable to the entire metropolitan area. In particular, the Hayward fault will gain in importance for a site in the East Bay, possibly changing the shape of the UHS. This strong spatial variation is probably less pronounced in Los Angeles and Sacramento.

Figures 5a to 5f compare the mean UHSs obtained from the hazard calculations to the UBC 94 (Category S_2) and NEHRP 94 (Categories C and D) spectra for the corresponding cities. The UBC 94 spectrum works well in Los Angeles (Figure 5a) but under-predicts intermediate- and long-period amplitudes in San Francisco (Figure 5c), where higher magnitudes contribute more to seismic hazard. The NEHRP 94 spectrum does not do much better in San Francisco because the NEHRP 94 maps have $A_a=A_V=0.4g$. A more appropriate value of A_V for San Francisco, together with the two anchor points used by the NEHRP 94 provisions, would provide an adequate fit. The comparisons for Sacramento (Figures 5e and 5f), suggest that the code values for this city are too high. This result should not be seen as conclusive because the source

characterization used here for Central California and the Sierra foothills is more crude than those used for the Los Angeles and San Francisco areas.

Figures 6a and 6b show comparisons in which the code shapes for Sacramento are anchored to values of PGA and S_a (1 sec) obtained from hazard results for rock (using the Youngs et al. and USGS sources mentioned earlier and the Abrahamson and Silva attenuation equations for rock). The UBC 94 spectral accelerations (Figures 6a) underestimate the UHS at all periods. The NEHRP 94 spectrum for Category D (the category most representative of the soil attenuation equations) is consistent with the UHS at some periods and is conservative at other periods.

CONCLUSIONS

In this project both spectral design shapes and the usefulness of two spectral anchors are investigated using a comprehensive strong motion database an updated empirical attenuation relation and current seismic-source characterizations. For the shapes, comparisons with statistical shapes with mean magnitudes in the range of 6.6 to 6.9 to design shapes suggest that both the UBC 94 and NEHRP 94 design spectra provide enveloping criteria (except for site D at short periods, $\leq$ 0.3 sec including cases for sites within 10 km of the fault rupture surface. For the NEHRP 94 design spectra, comparison of the F_a and F_v factors to those implied by a recently developed empirical attenuation relation suggest that the NEHRP 94 F_a factors may reflect too little nonlinearity while the F_v factors may show too much nonlinearity.

Comparison of the code spectral shapes to the results from the probabilistic analysis (for 90% non-exceedence probability in 50 years) show that the fixed UBC 94 shape underestimates intermediate-to-long period amplitudes ($T \geq 1$ sec) in San Francisco by about 25% due to the contribution of large magnitude earthquakes ($M > 7$), is adequate in Los Angeles, and significantly overestimates the hazard in Sacramento. The NEHRP 94 spectrum does slightly better in San Francisco but is still inadequate at intermediate-to-long periods. A larger value of A_v ($A_v = 0.4g$ for San Francisco in the NEHRP 94 maps) would provide more adequate design values. For Sacramento, anchoring the UBC 94 and NEHRP 94 code provision shapes to rock hazard results produces UBC 94 shapes which underestimate the hazard up to 50%. The more flexible NEHRP 94 shape allows for a better fit to the probabilistic results, but only if both anchoring values (A_a and A_v) are specified in a manner consistent with the seismic hazard.

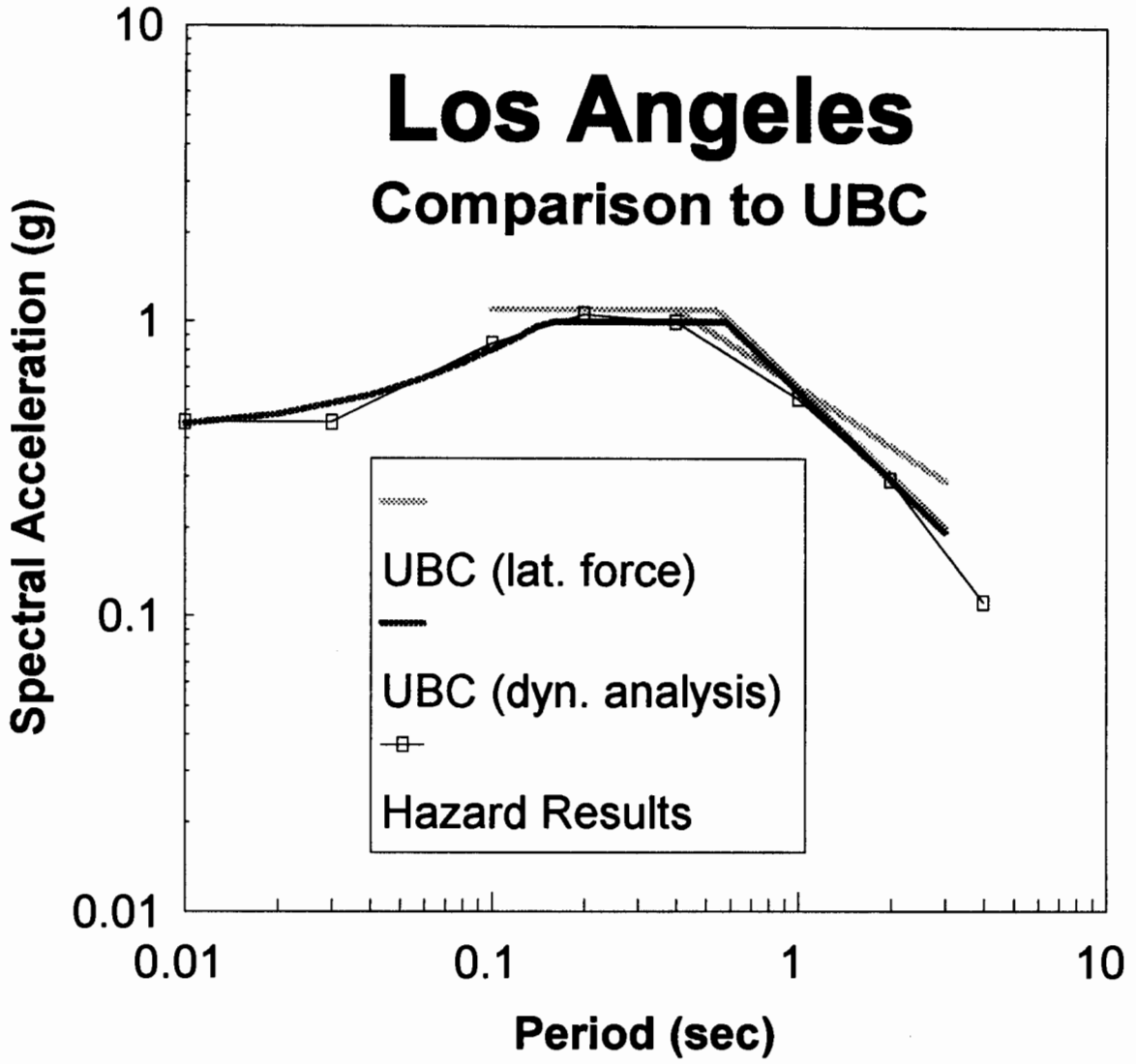

Figure 5a. Comparison of UBC 94 spectra to the corresponding mean uniform-hazard spectra for 90% non-exceedence probability in 50 years for downtown Los Angeles.

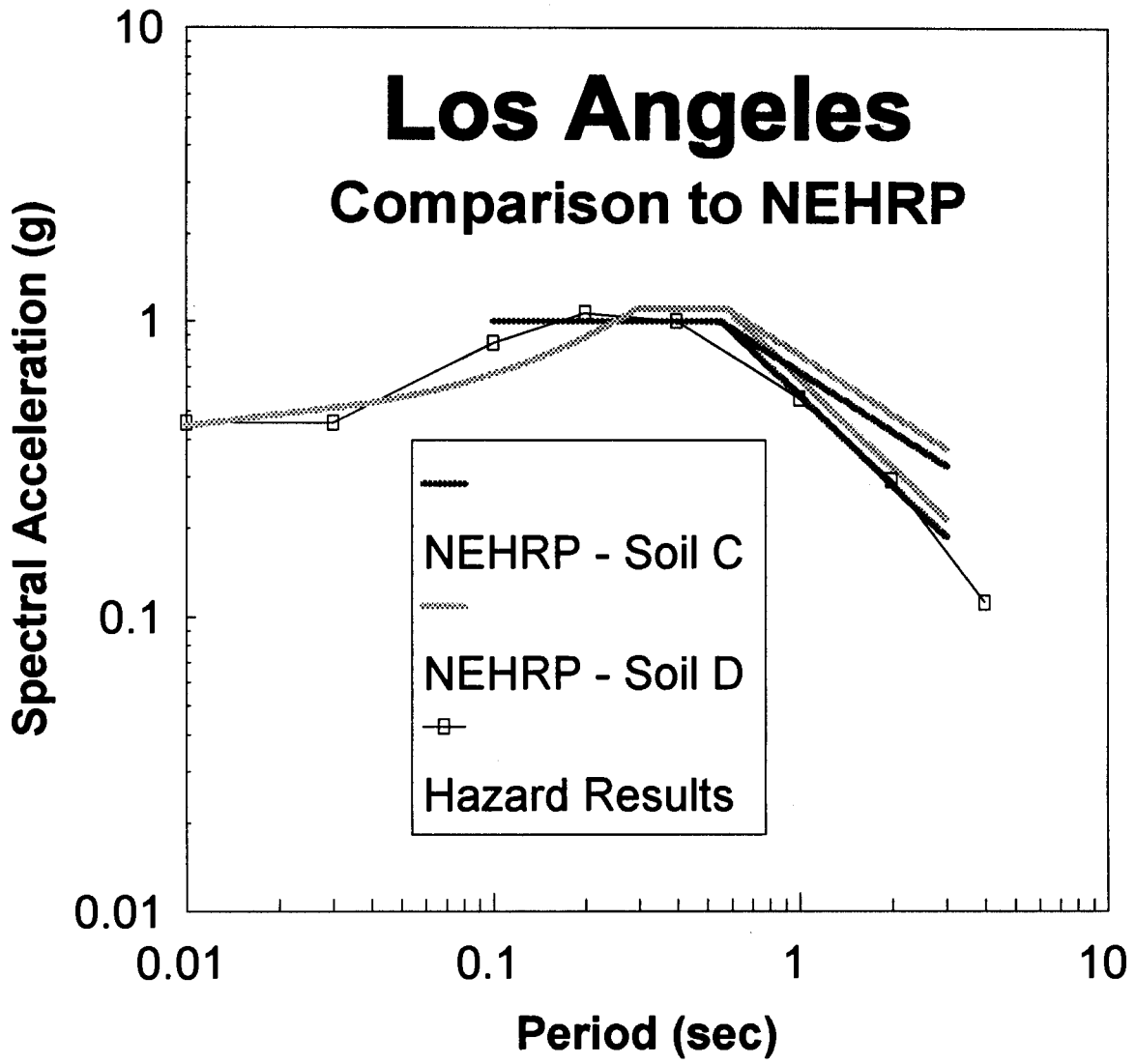

Figure 5b. Comparison of NEHRP 94 spectra to the corresponding mean uniform-hazard spectra for 90% non-exceedence probability in 50 years for downtown Los Angeles.

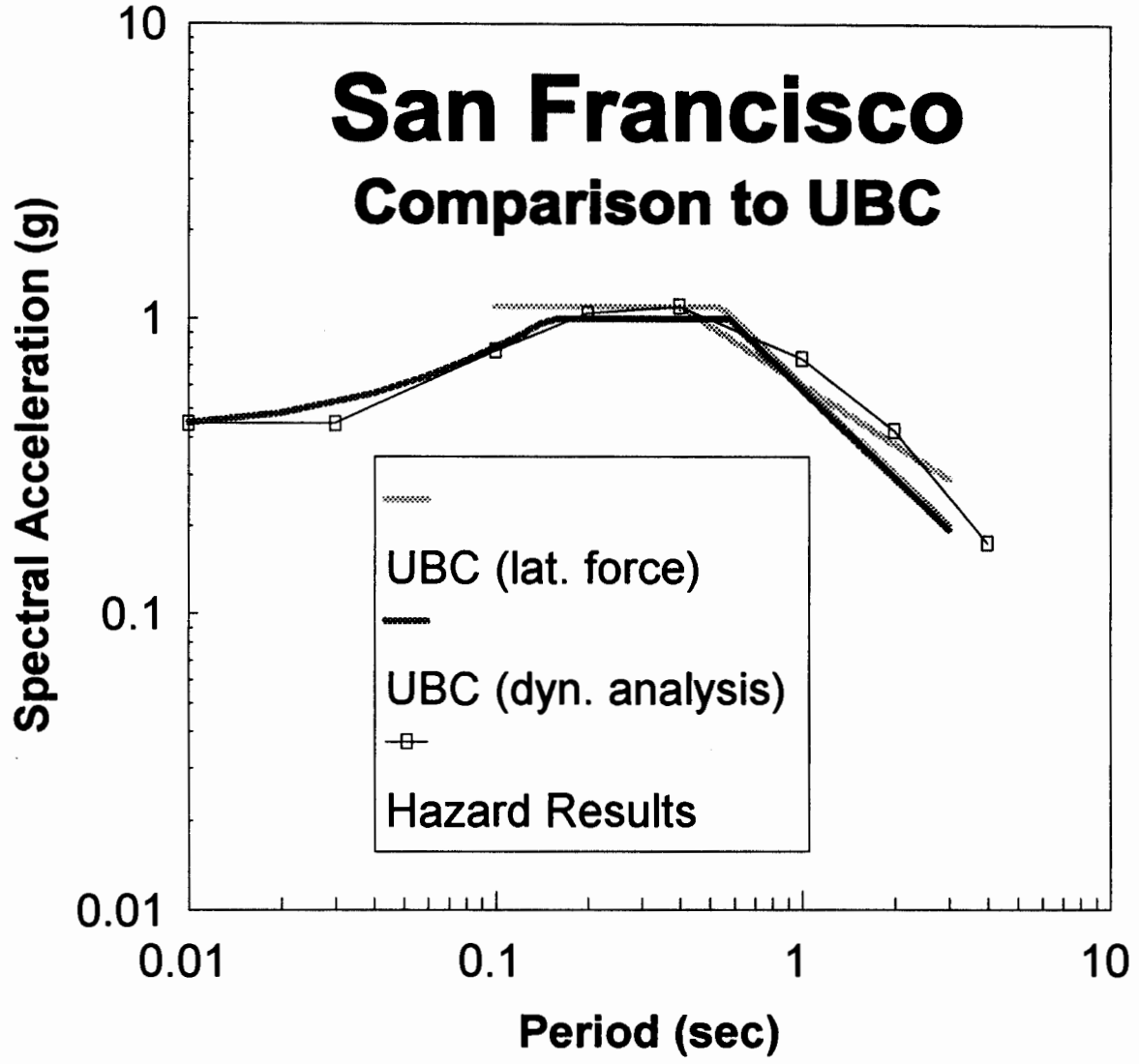

Figure 5c. Comparison of UBC 94 spectra to the corresponding mean uniform-hazard spectra for 90% non-exceedence probability in 50 years for the San Francisco financial district.

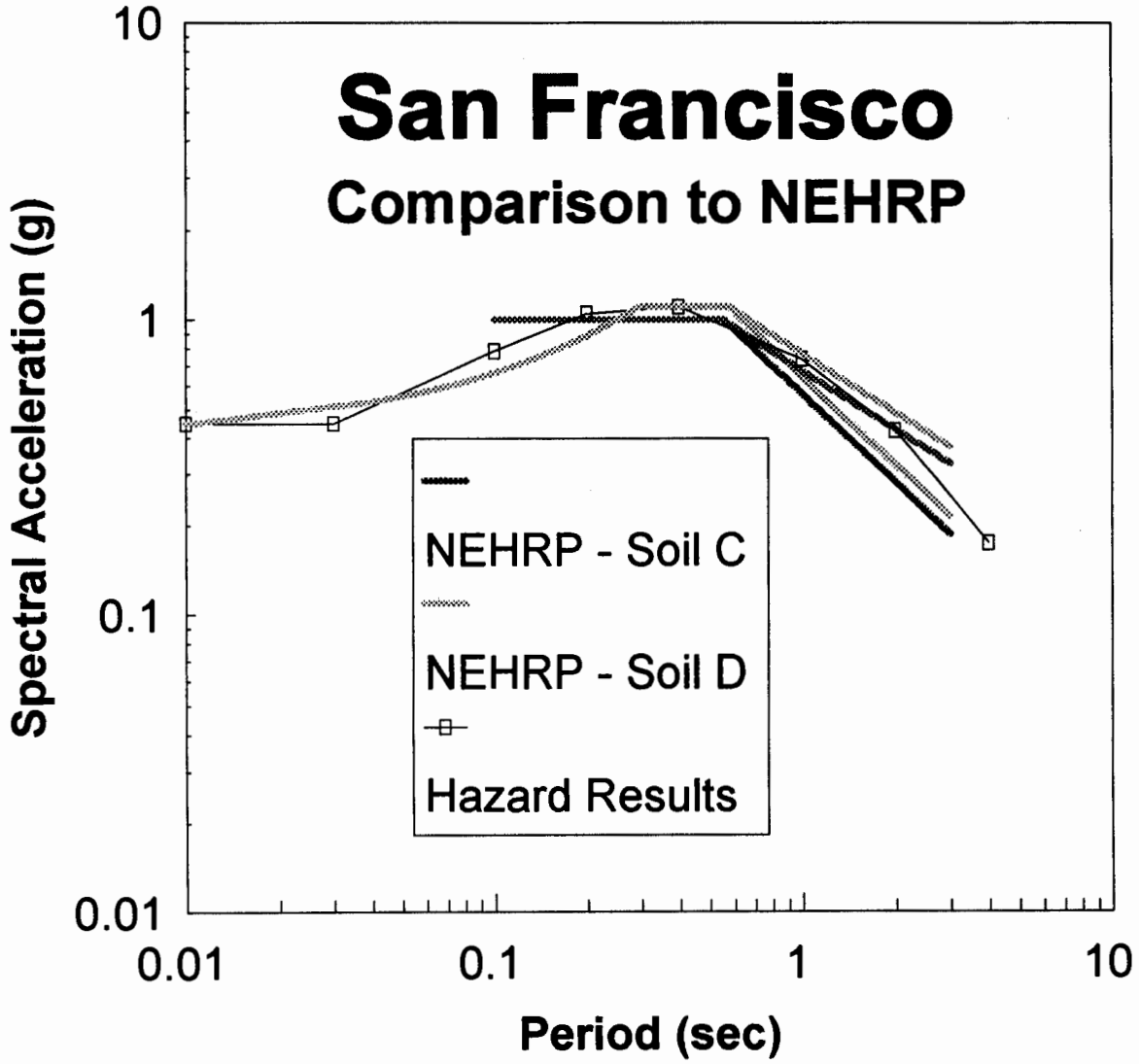

Figure 5d. Comparison of NEHRP 94 spectra to the corresponding mean uniform-hazard spectra for 90% non-exceedence probability in 50 years for the San Francisco financial district.

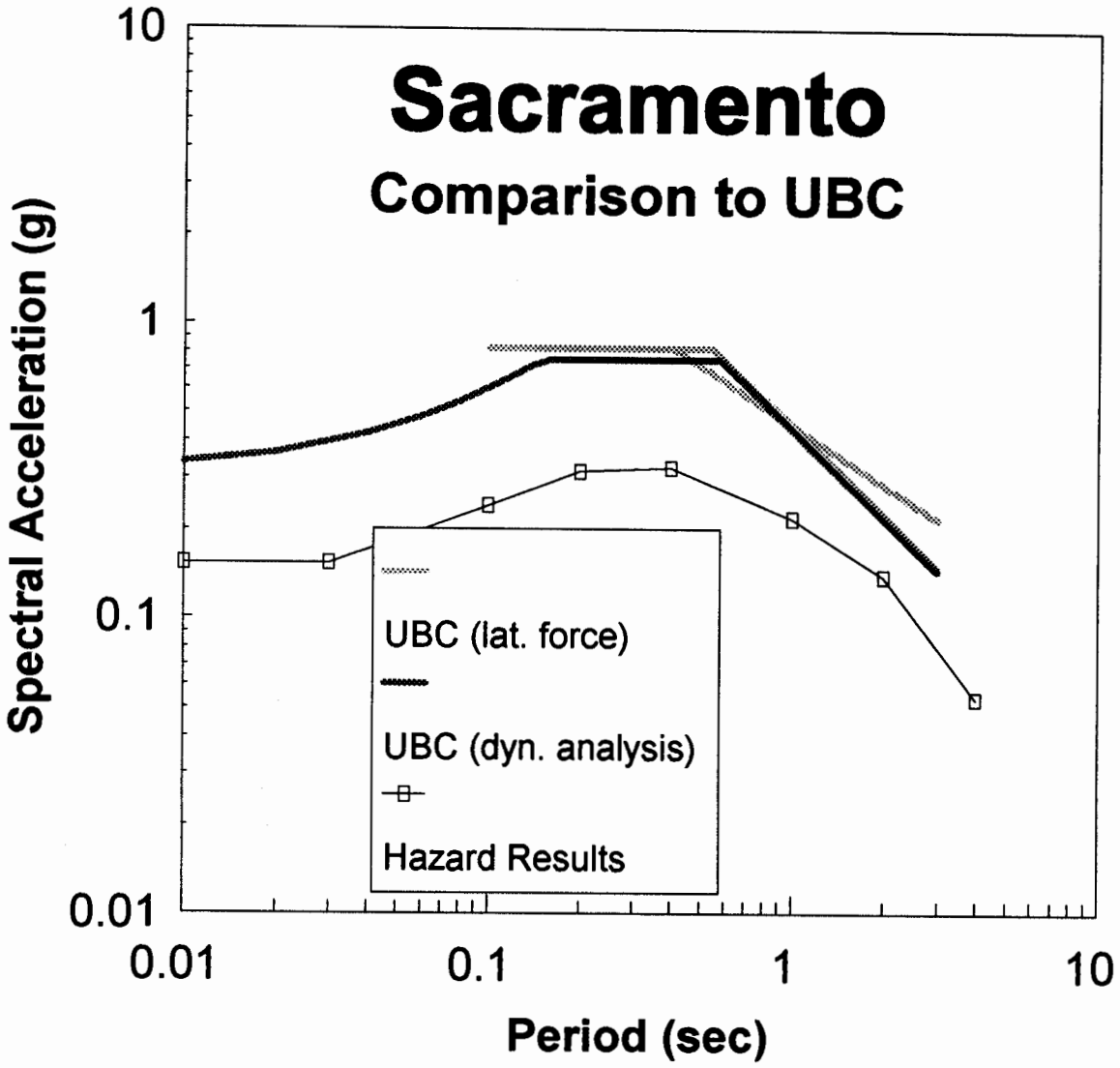

Figure 5e. Comparison of UBC 94 spectra to the corresponding mean uniform-hazard spectra for 90% non-exceedence probability in 50 years for Sacramento.

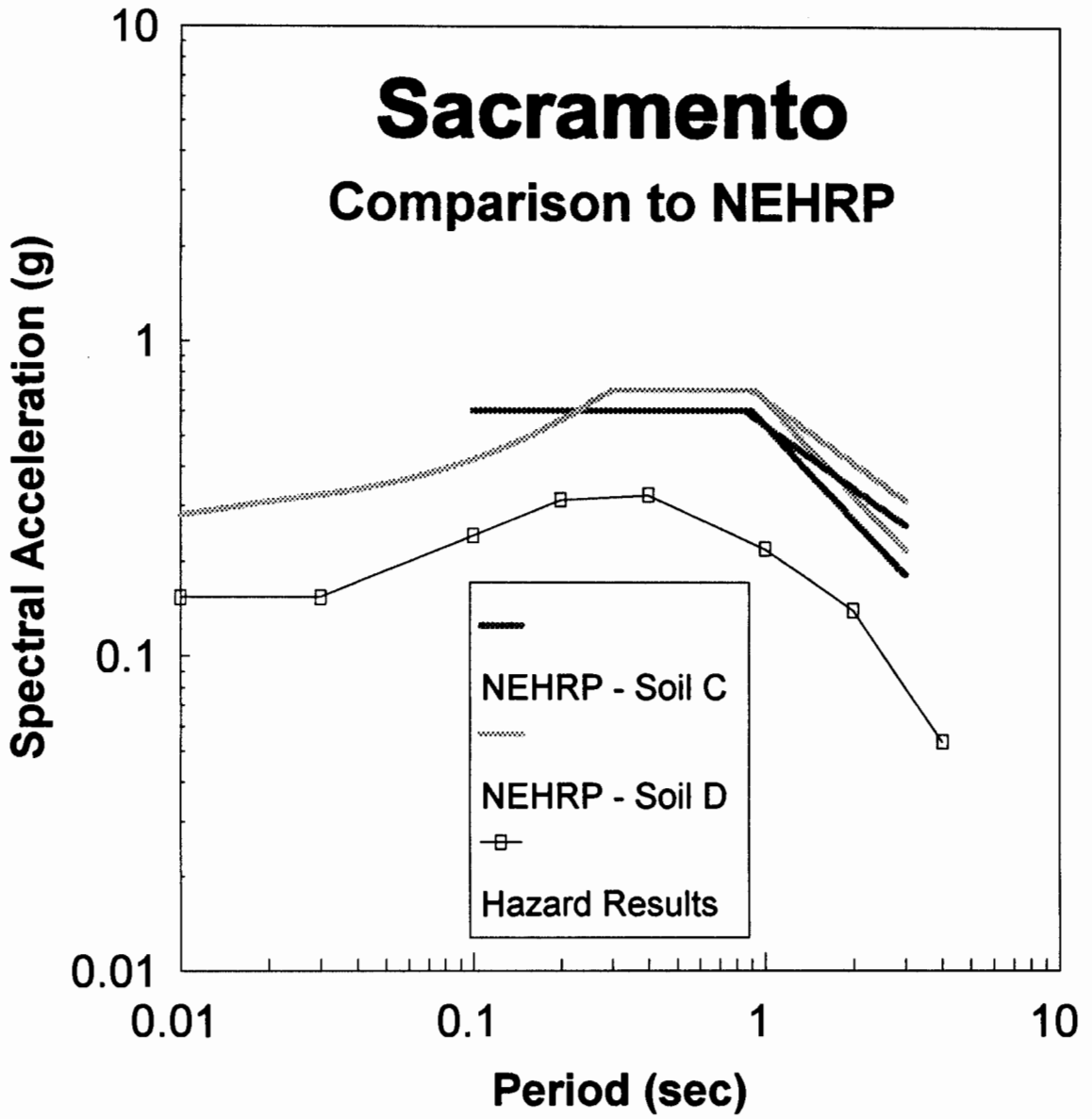

Figure 5f. Comparison of NEHRP 94 spectra to the corresponding mean uniform-hazard spectra for 90% non-exceedence probability in 50 years for Sacramento.

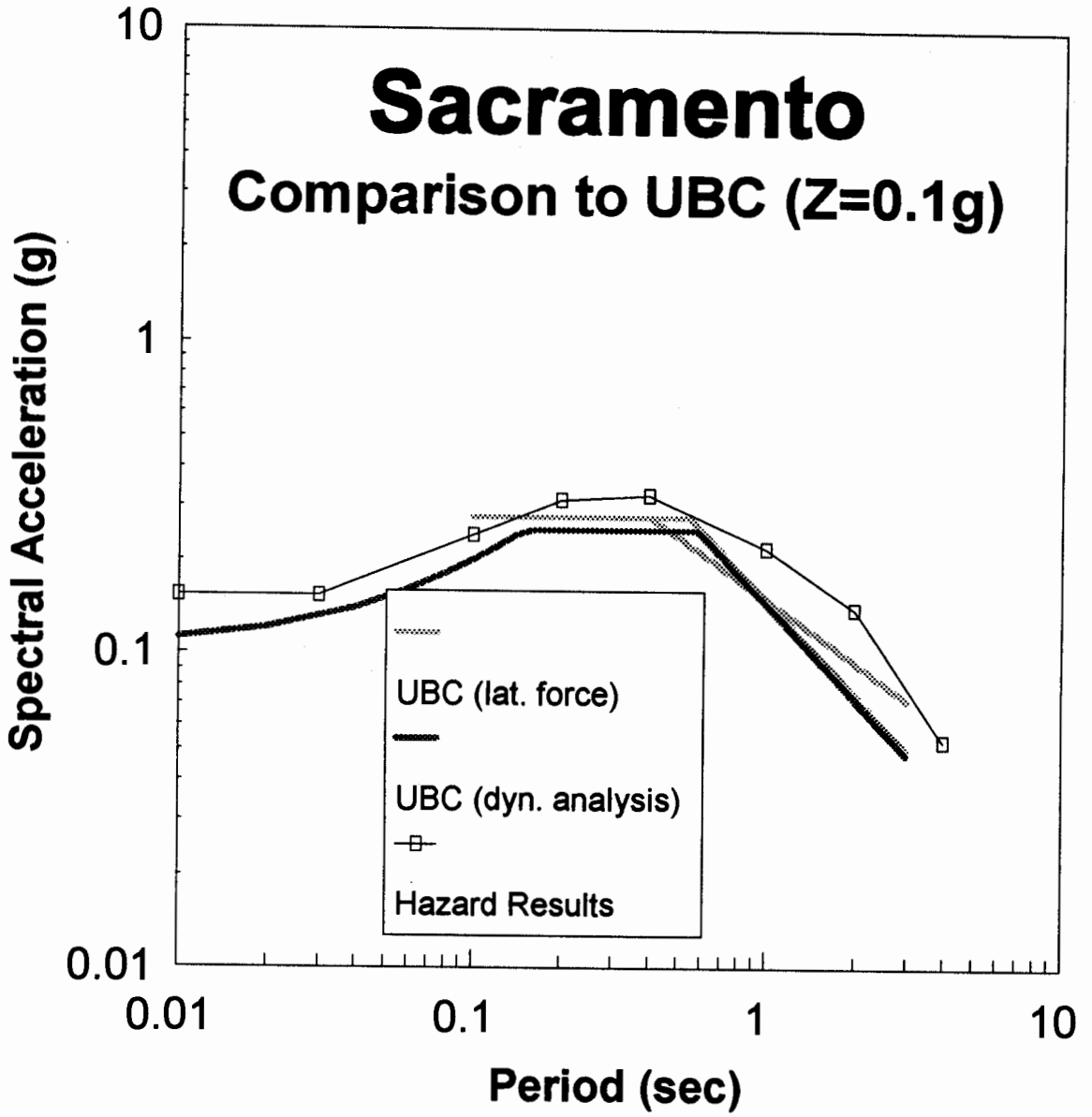

Figure 6a. Comparison of UBC 94 spectra for Sacramento to the corresponding mean uniform-hazard spectra for 90% non-exceedence probability in 50 years. Code shapes are anchored to rock seismic-hazard results.

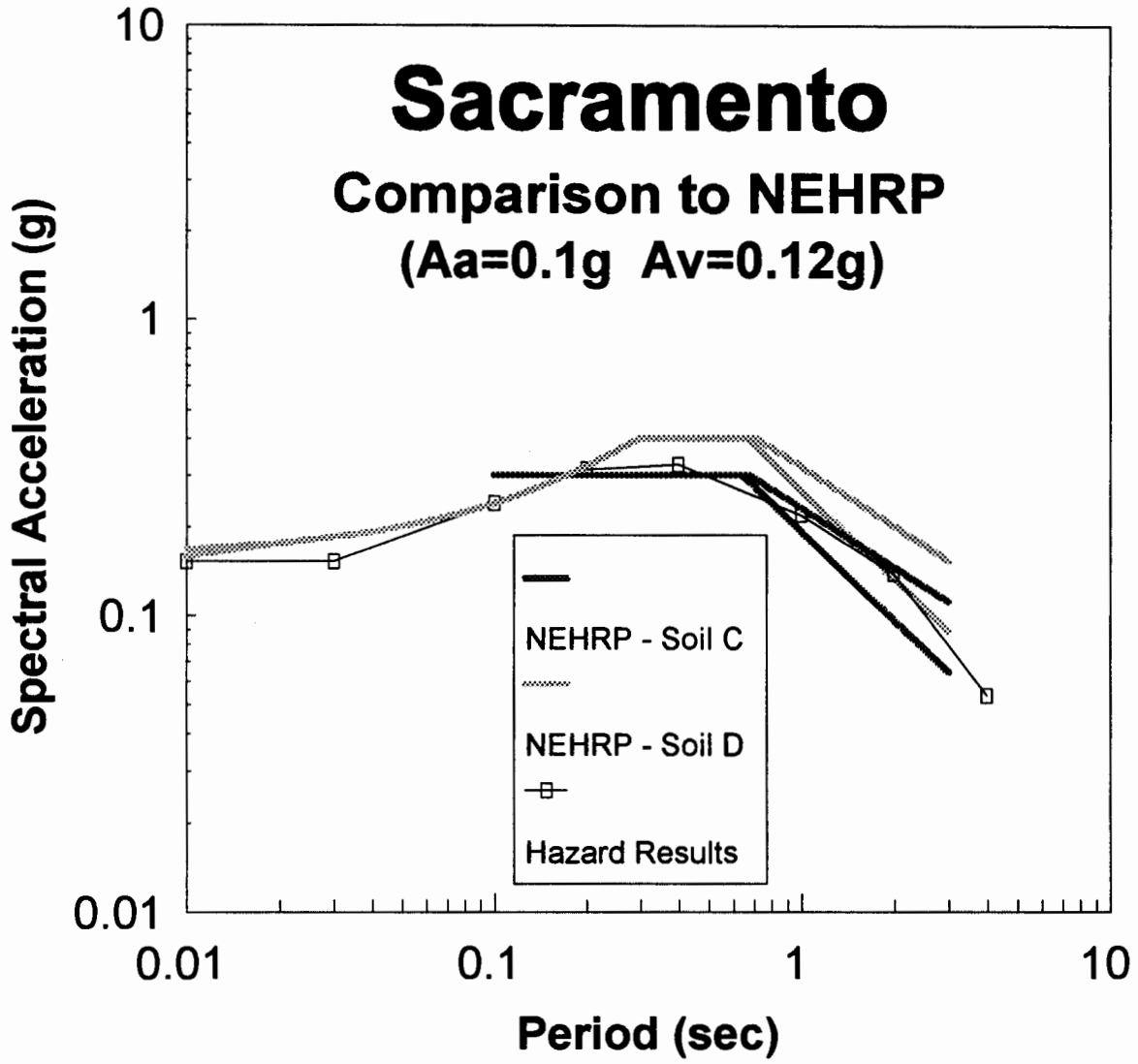

Figure 6b. Comparison of NEHRP 94 spectra for Sacramento to the corresponding mean uniform-hazard spectra for 90% non-exceedence probability in 50 years. Code shapes are anchored to rock seismic-hazard results.

REFERENCES

Abrahamson, N.A. and Silva, W.J. (1997). "Empirical response spectral attenuation relations for shallow crustal earthquakes." *Seismological Research Let.*, 68(1), 94-127.

Boore, D.M., W.B. Joyner, and T.E. Fumal (1994). "Estimation of response spectra and peak accelerations from western North American earthquakes: and interim report. Part 2. *U.S. Geological Survey Open-File Rept.* 94-127.

Borcherdt, R. D. (1994). "Estimates of site-dependent response spectra for design (methodology and justification). *Earthquake Spectra,* 10(4), 617-653.

Crouse, C. B. and McGuire, J.W. (1996). "Site response studies for purpose of revising NEHRP seismic provisions." *Earthquake Spectra,* 12(3), 407-439.

Frankel, A., C. Mueller, T. Barnhard, D. Perkins, E.V. Leyendecker, N. Dickman, S. Hanson, and M. Hopper (1995). "Interim National Seismic Hazard Maps." Internet Web Page, December 15.

Hansen, S. and D. Perkins (1985). *Seismic Sources and Recurrence Rates as Adopted by USGS Staff for the Production of the 1982 and 1990 Probabilistic Ground Motion Maps for Alaska and the Conterminious United States*. USGS Open-file Report 95-257.

McGuire, R.K. (1995). "Probabilistic Seismic Hazard Analysis and Design Earthquakes: Closing the Loop," *Bull., Seism. Soc. Am.*, 85(5).

Mohraz, B. (1976). "A study of earthquake response spectra for different geological conditions." *Bull. Seism. Soc. Am.*, 66(3) 915-935.

Petersen, M.D., C.H. Cramer, W.A. Bryant, M.S. Reichle, and T.R. Toppozada (1995). "Preliminary seismic Hazard Assessment for Los Angeles, Ventura and Orange counties, California Affected by the the January 17, 1994 Northridge Earthquake." *Bull. Seism. Soc. Am*, 86(1b), 5247-5261.

Sadigh (1988). Written 1987 Communication to W. Joyner. Published in Joyner, W.B., and Boore, D.M., "Measurement, characterization, and prediction of Ground Motion," Proc. Conf. on Earthquake Engineering and Soil Dynamics II, GT Div., *ASCE*, pp. 43-102.

Seed, H.B., C. Ugas and J. Lysmer. (1976). "Site-dependent spectra for earthquake resistant design." *Bull. Seism. Soc. Am.*, 66(1), 221-243.

Working Group on California Earthquake Probabilities (1990). *Probabilities of Large Earthquakes in the San Francisco Bay Region, California.* USGS Circular 1053.

Working Group on California Earthquake Probabilities (1995). "Seismic Hazards in Southern California: Probable Earthquakes , 1994 to 2024," *Bull., Seism. Soc. Am.*, v. 85, no. 2.

Youngs, R.R, K.J. Coppersmith, C.L. Taylor, M.S. Power, L.A. DiSilvestro, M.L. Angell, N.T. Hall, J.R. Wesling, and L. Mualchin (1992). "A comprehensive Seismic Hazard Model for the San Francisco Bay Area." in *Proc., Second Conference on Earthquake Hazards in the Eastern San Francisco Bay Area*, California Division of Mines and Geology, Special Publication 113.

LIST OF CSMIP DATA UTILIZATION REPORTS

California Department of Conservation
Division of Mines and Geology
Office of Strong Motion Studies
California Strong Motion Instrumentation Program (CSMIP)

The California Strong Motion Instrumentation Program (CSMIP) publishes data utilization reports as part of the Data Interpretation Project. These reports were prepared by investigators funded by CSMIP. Results obtained by the investigators were summarized in the papers included in the proceedings of the annual seminar. These reports and seminar proceedings are available from CSMIP at nominal cost. Requests for the reports, seminar proceedings and/or for additional information should be addressed to: Data Interpretation Project Manager, Office of Strong Motion Studies, Division of Mines and Geology, California Department of Conservation, 801 K Street, MS 13-35, Sacramento, California 95814-3531. Phone: (916)322-3105

CSMIP/92-01 **"Evaluation of Soil-Structure Interaction in Buildings during Earthquakes,"** by G. Fenves and G. Serino, June 1992, 57 pp.

CSMIP/92-02 **"Seismic Performance Investigation of the Hayward BART Elevated Section,"** by W. Tseng, M. Yang and J. Penzien, September 1992, 61 pp.

CSMIP/93-01 **"Influence of Critical Moho Reflections on Strong Motion Attenuation in California,"** by P. Somerville, N. Smith and D. Dreger, December 1993, 84 pp.

CSMIP/93-02 **"Investigation of the Response of Puddingstone Dam in the Whittier Narrows Earthquake of October 1, 1987,"** by J. Bray, R. Seed and R. Boulanger, December 1993, 60 pp.

CSMIP/93-03 **"Investigation of the Response of Cogswell Dam in the Whittier Narrows Earthquake of October 1, 1987,"** by R. Boulanger, R. Seed and J. Bray, December 1993, 53 pp.

CSMIP/94-01 **"Torsional Response Characteristics of Regular Buildings under Different Seismic Excitation Levels,"** by H. Sedarat, S. Gupta, and S. Werner, January 1994, 43 pp.

CSMIP/94-02 **"Degradation of Plywood Roof Diaphragms under Multiple Earthquake Loading,"** by J. Bouwkamp, R. Hamburger and J. Gillengerten, February 1994, 32 pp.

CSMIP/94-03 **"Analysis of the Recorded Response of Lexington Dam during Various Levels of Ground Shaking,"** by F. Makdisi, C. Chang, Z. Wang and C. Mok, March 1994, 60 pp.

LIST OF CSMIP DATA UTILIZATION REPORTS (continued)

CSMIP/94-04 **"Correlation between Recorded Building Data and Non-Structural Damage during the Loma Prieta Earthquake of October 17, 1989,"** by S. Rihal, April 1994, 65 pp.

CSMIP/94-05 **"Simulation of the Recorded Response of Unreinforced Masonry (URM) Infill Buildings,"** by J. Kariotis, J. Guh, G. Hart and J. Hill, October 1994, 149 pp.

CSMIP/95-01 **"Seismic Response Study of the Hwy 101/Painter Street Overpass Near Eureka Using Strong-Motion Records,"** by R. Goel and A. Chopra, March 1995, 70 pp.

CSMIP/95-02 **"Evaluation of the Response of I-10/215 Interchange Bridge Near San Bernardino in the 1992 Landers and Big Bear Earthquakes,"** by G. Fenves and R. Desroches, March 1995, 132 pp.

CSMIP/95-03 **"Site Response Studies for Purpose of Revising NEHRP Seismic Provisions,"** by C.B. Crouse, March 1995, 68 pp.

CSMIP/96-01 **"An Investigation of UBC Serviceability Requirements from Building Responses Recorded During the 1989 Loma Prieta Earthquake,"** by C.-M. Uang and A. Maarouf, September 1996, 140 pp.

CSMIP/96-02 **"Evaluation of Displacement Amplification Factor for Seismic Design Provisions,"** by C.-M. Uang and A. Maarouf, September 1996, 167 pp.

CSMIP/00-01 **"Prediction of Ground Motions for Thrust Earthquakes,"** by P. Somerville and N. Abrahamson, February 2000, 56 pp.

CSMIP/00-02 **"Quantifying the Effect of Soil-Structure Interaction for Use in Building Design,"** by C. Poland, J. Soulages, J. Sun and L. Mejia, February 2000, 99 pp.

CSMIP/00-03 **"Seismic Performance and Design Considerations of Long Span Suspension Bridges,"** by W.D. Liu, A. Kartoum, K. Chang and R. Imbsen, February 2000, 132 pp.

CSMIP/00-04 **"Analyses of Strong-Motion Records from a Parking Structure during the 17 January 1994 Northridge Earthquake,"** by S. Hilmy, S. Werner, A. Nisar and J. Beck, March 2000, 117 pp.

CSMIP/00-05 **"Effect of Contraction Joint Opening on Pacoima Dam in the 1994 Northridge Earthquake,"** by S. Mojtahedi and G. Fenves, March 2000, 87 pp.

LIST OF CSMIP DATA UTILIZATION REPORTS (continued)

CSMIP/00-06 **"Verification of Response Spectral Shapes and Anchor Points for Different Site Categories in Building Design Codes,"** by W. Silva and G. Toro, March 2000, 48 pp.

SMIP89 "SMIP89 Seminar on Seismological and Engineering Implications on Recent Strong-motion Data," Preprints, Sacramento, California, May 9, 1989

SMIP90 "SMIP90 Seminar on Seismological and Engineering Implications on Recent Strong-motion Data," Preprints, Sacramento, California, June 8, 1990

SMIP91 "SMIP91 Seminar on Seismological and Engineering Implications on Recent Strong-motion Data," Preprints, Sacramento, California, May 30, 1991

SMIP92 "SMIP92 Seminar on Seismological and Engineering Implications on Recent Strong-motion Data," Proceedings, Sacramento, California, May 21, 1992

SMIP93 "SMIP93 Seminar on Seismological and Engineering Implications on Recent Strong-motion Data," Proceedings, Sacramento, California, May 20, 1993, 114 pp.

SMIP94 "SMIP94 Seminar on Seismological and Engineering Implications on Recent Strong-motion Data," Proceedings, Los Angeles, California, May 26, 1994, 120 pp.

SMIP95 "SMIP95 Seminar on Seismological and Engineering Implications on Recent Strong-motion Data," Proceedings, San Francisco, California, May 16, 1995, 105 pp

SMIP96 "SMIP96 Seminar on Seismological and Engineering Implications on Recent Strong-motion Data," Proceedings, Sacramento, California, May 14, 1996, 130 pp.

SMIP97 "SMIP97 Seminar on Utilization of Strong-Motion Data," Proceedings, Los Angeles, California, May 8, 1997, 127 pp.

SMIP98 "SMIP98 Seminar on Utilization of Strong-Motion Data," Proceedings, Oakland, California, September 15, 1998, 175 pp.

SMIP99 "SMIP99 Seminar on Utilization of Strong-Motion Data," Proceedings, Los Angeles, California, September 15, 1999, 154 pp.